Chapter B.3

The Cooke Triplet and Tessar Lenses

Following the introduction of photography in 1839, the development of camera lenses progressed in an evolutionary way with occasional revolutions. Almost immediately, the singlet meniscus Landscape lens was achromatized, thus becoming a cemented doublet meniscus. Soon afterward, pairs of either singlet or doublet menisci were combined symmetrically about a stop. The most successful of the double-doublets was the Rapid Rectilinear lens, introduced in 1866. This use of symmetry was then further extended to pairs of menisci, with each meniscus consisting of three, four, or even five elements cemented together. The most successful of these lenses was the Dagor, a double-triplet (six elements), introduced in 1892. The Dagor and some of its variants are still in use today.

The first revolution or major innovation occurred in 1840 by Joseph Petzval with his introduction of mathematically designed lenses. Petzval's most famous lens is the Petzval Portrait lens. The Petzval lens is not symmetrical and has major aberrations off-axis (most noticeably, field curvature). Nevertheless, in 1840 it was an immediate success, not least because at *f*/3.6 it was 20 times faster (transmitted 20 times more light) than the *f*/16 Landscape lens, its only competition at the time. Petzval type lenses were widely used until well into the twentieth century, and they are sometimes still encountered, especially in projectors.

The second revolution, which began in 1886, was the development of new types of optical glass, especially the high-index crowns. These glasses made possible the first anastigmatic lenses; that is, lenses with astigmatism corrected on a flat field.

The third revolution was the invention by H. Dennis Taylor in 1893 of the Cooke Triplet lens (Cooke was Taylor's employer). A Cooke Triplet consists of two positive singlet elements and one negative singlet element, all of which can be thin. Two sizable airspaces separate the three elements. The negative element is located in the middle about halfway between the positive elements, thus maintaining a large amount of symmetry. By this approach, Taylor found that he could accomplish with only three elements what others required six, eight, or ten ele-

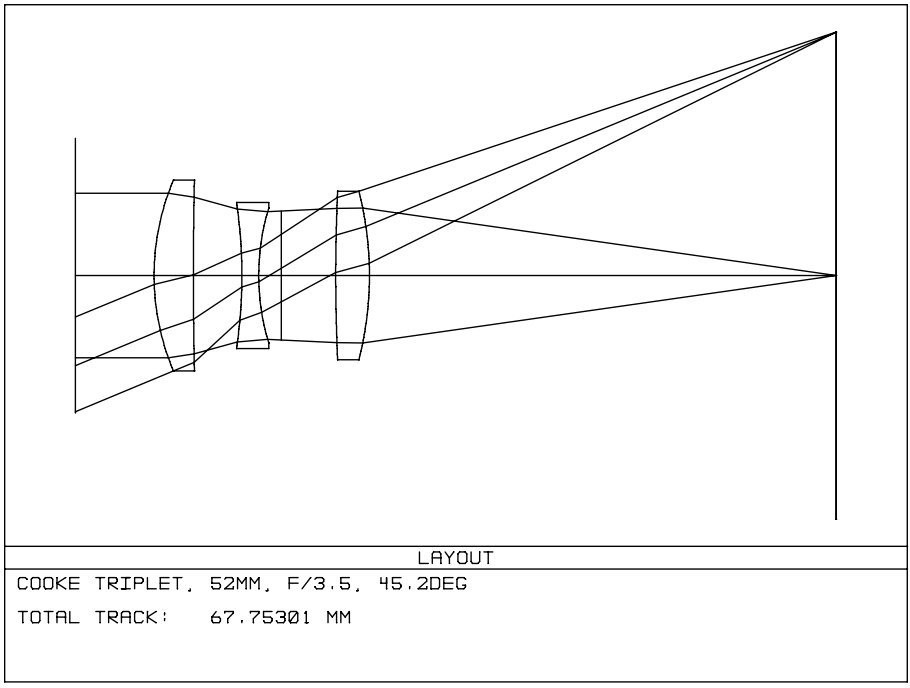

Figure B.3.1.1

ments to do when using pairs of cemented menisci. After more than a century, the Cooke Triplet remains one of the most popular camera lens forms.

The design and performance of a Cooke Triplet is the main subject of this chapter. The construction of a Cooke Triplet is illustrated in Figure B.3.1.1. Also included here for comparison is a Tessar lens, which can be considered a derivative and extension of the Cooke Triplet (although Paul Rudolph designed the first Tessar in 1902 as a modification of an earlier anastigmat, the Protar).

The development of camera lenses has continued unabated to this day, with a huge number of evolutionary advances and several more revolutions (most notably, anti-reflection coatings and computer-aided optimization). The reader is encouraged to become familiar with optical history. It is a fascinating story.[1]

B.3.1 Lens Specifications

The lenses in this chapter are normal or standard lenses for a 35 mm type still (not movie) camera with the object at infinity. Note that 35 mm refers to the phys-

[1] Optical history is discussed in many of the references listed in the bibliography. Three particularly good sources are: Rudolf Kingslake, *A History of the Photographic Lens*; Henry C. King, *The History of the Telescope*; and Joseph Ashbrook, *The Astronomical Scrapbook.*

ical width of the film, not to the image size, which is only 24 mm wide (and 36 mm long). This image size was chosen for the first Leica camera in 1924 and has been the standard ever since. The remaining film area is occupied by two sets of sprocket holes, a vestige from its origin as a motion picture film (where the image is only 18 mm long).

As mentioned in the previous chapter, a normal lens gives normal-perspective photographs and has a focal length roughly equal to the image format diameter or diagonal. At 24x36 mm, the diagonal of the 35 mm format is 43.3 mm. However, the lens on the first Leica had a focal length of 50 mm, and again this value has become standard. Actually, most normal lenses for 35 mm cameras are deliberately designed to have a focal length even a bit longer still. Thus, although the nominal focal length engraved on the lens barrel is 50 mm, the true focal length is often closer to 52 mm. Thus, 52.0 mm is adopted as the focal length for the lenses in this chapter. This focal length is longer than the format diagonal, but it is close enough.

Given this focal length and image format, the diagonal field of view (from corner to corner) is 45.2º, or ±22.6º. Four field positions are used during optimization and evaluation: 0º, 9º, 15.8º, and 22.6º (or 0, 40%, 70%, and 100% of half-field). Object 1 is in the field center, object 4 is at the distance of the format corner, object 3 is at the distance of one side of an equivalent square format, and object 2 is slightly greater than halfway between objects 1 and 3. Of course, for an ordinary camera lens, the field (image surface) is flat.

For a photographic Cooke Triplet covering this angular view, it is usually not practical to increase speed beyond about *f*/3.5. Triplets with focal lengths of 52 mm and speeds of *f*/3.5 are widely manufactured and used with success. Thus, *f*/3.5 is adopted here.

During optimization, no special emphasis is given to the center of the pupil to the detriment of the pupil edges. To increase performance when stopped down, the lens is optimized and used on the paraxial focal plane. At the edge of the field, a reasonable amount of mechanical vignetting is allowed. Distortion is corrected to zero at the edge of the field.

Five wavelengths are used during optimization and evaluation. Because most films are sensitive to wavelengths between about 0.40 μm and 0.70 μm, the five wavelengths are: 0.45, 0.50, 0.55, 0.60, and 0.65 μm. For panchromatic film sensitivity, these wavelengths are weighted equally. The reference wavelength for calculating first-order properties and solves is the central wavelength, 0.55 μm.

And finally, the performance criterion for the optimized lens is diffraction MTF; that is, the form of MTF with both diffraction and aberrations included.

B.3.2 Degrees of Freedom

The Cooke Triplet is a very interesting optical configuration.[2] Refer again to

Figure B.3.1.1. There are exactly eight effective independent variables or degrees of freedom available for the control of optical properties. These major variables are six lens surface curvatures and two interelement airspaces. The six curvatures can also be viewed as three lens powers and three lens bendings.

Recall that there are seven basic or primary aberrations (first-order longitudinal and lateral color, and the five monochromatic third-order Seidel aberrations). Thus, the Cooke Triplet has just enough effective independent variables to correct all first- and third-order aberrations plus focal length.

Although the airspaces in a Cooke Triplet are effective variables, the glass thicknesses are unfortunately only weak, ineffective variables that somewhat duplicate the airspaces. The glass center thicknesses are usually arbitrarily chosen for ease of fabrication.

The three glass choices can also be viewed as variables (or index and dispersion variable pairs). But the range of available glasses is limited, and the requirements of achromatization further restrict the glasses. In practice, the role of glass selection is to determine which of a multitude of possible optical solutions you get.

Stop shift is not a degree of freedom. A Cooke Triplet is nearly symmetrical about the middle element, which makes aberration control much easier. To retain as much symmetry as possible, the stop is either at the middle element or just to one side. A slightly separated stop allows the stop to be a variable iris diaphragm for changing the *f*/number. Locating the iris to the rear of the middle element, rather than to the front, is more common, although both work. In the present example, the stop is 2 mm behind the middle element.

With only eight effective variables, there are no variables available for controlling the higher-order monochromatic aberrations that will inevitably be present. Although it is possible in a Cooke Triplet to correct all seven first- and third-order aberrations exactly to zero, in practice this is never done. Controlled amounts of third-order aberrations are always deliberately left in to balance the fifth- and higher-orders. However, there is a limit to how well this cancellation works. Thus, Cooke Triplets are usually restricted to applications requiring only moderate speed and field coverage; that is, where there are only moderate amounts of fifth- and higher-order aberrations. For higher performance, a lens configuration with a larger number of effective degrees of freedom is needed.

[2] For those interested in the more analytical aspects of designing a Cooke Triplet lens, see the excellent discussions in: Warren J. Smith, *Modern Optical Engineering*, second edition, pp. 384-390; Warren J. Smith, *Modern Lens Design*, pp. 123-146; and Rudolf Kingslake, *Lens Design Fundamentals*, pp. 286-295. These three books are also highly recommended for their discussions of many other topics in optics.

B.3.3 Glass Selection

A Cooke Triplet is an achromat. Thus, as discussed in Chapter B.1, each of the two positive elements must be made of a crown type glass (lower dispersion or higher Abbe number), and the negative element must be made of a flint type glass (higher dispersion or lower Abbe number).

For practical reasons, and with no loss of performance, both positive crown elements are usually made of the same glass type, and this will be done here.

The sizes of the airspaces in a Cooke Triplet are a strong function of the dispersion difference between the crown and flint glasses. A dispersion difference that is too small causes the lens elements to be jammed up against each other, and there are also large aberrations. Conversely, a dispersion difference that is too large causes the system to be excessively stretched out, and again there are large aberrations. One value of dispersion difference produces airspaces of the right size to yield a good optical solution. Fortunately, the required dispersion difference can be satisfied by the range of actual available glasses on the glass map.

The difference in n_d index of refraction between the crown and flint glasses also enters into the optical solution. To help reduce the Petzval sum to flatten the field, the positive elements should be made of a higher-index crown glass, and the negative element should be made of a somewhat lower-index flint glass.

To make this an exercise in determining the capability of the Cooke Triplet design form, all the more or less normal glass types will be allowed. This includes all the expensive high-index lanthanum glasses. Glass cost should not be a driving issue here because the lens elements are quite small and require only small amounts of glass. Optical and machine shop fabrication costs should be much more important than glass cost. However, this is not true for all types of lenses; the relative importance of glass cost gets greater as element sizes get larger. Note that no attempt is made here to reduce secondary color, and thus the abnormal-dispersion glasses are excluded.

Experience has shown that high-index crown glasses generally give better image quality. Not only is the Petzval sum reduced, but high indices yield lower surface curvatures that in turn reduce the higher-order aberrations. Because there are relatively few high-index crowns on the glass map, the usual procedure when selecting glasses for a Cooke Triplet is to first select the crown glass type, and to then select the matching flint glass type from among the many possibilities.

Refer back to the glass map in Figure A.10.2. Note that the boundary of the highest-index crowns is a nearly straight line on the upper left side extending from (in the Schott catalog) about SK16 (n_d of 1.620, V_d of 60.3) to about LaSFN31 (n_d of 1.881, V_d of 41.0). Although the top of this line extends well into the nominally flint glasses, the glasses along the top can function as crown glasses because they are more crowny than the very flinty dense SF glasses with which they would be paired.

The candidate crown glasses are therefore located along the line bounding the upper left of the populated region of the glass map. An excellent crown glass of very high index is Schott LaFN21 (n_d of 1.788, V_d of 47.5). Although not the most extreme high-index crown, LaFN21 is widely used and practical. Thus, LaFN21 is adopted here.

Given the crown glass selection, the basic optical design requires a matching flint having a certain dispersion difference and a low index. However, there is a limit to how low the flint index can be. This limit is the arc bordering the right and bottom of the populated region of the glass map (again see Figure A.10.2). This arc is called the old glass line. Thus, it is from the glasses along the old glass line that the flint glass of a Cooke Triplet is usually selected.

For early optimizations, make a guess at the flint glass type. Fortunately, your guess does not have to be very good because it will soon be revised. Accordingly, Schott SF15 (n_d of 1.699, V_d of 30.1), a glass on the old glass line with an index somewhat lower than LaFN21, is provisionally adopted.

For intermediate optimizations, the same crown glass selection, LaFN21, is retained, but a more optimum flint glass match must now be made. One way to find the best flint is to let flint glass type be a variable during optimization and let the computer make the selection. However, because some lens design programs may have difficulty handling variable glasses, a manual approach may be more effective, and also more revealing to the lens designer.

Using the manual approach, select several likely flint glass candidates from along the old glass line to combine with LaFN21. For each combination, optimize the Cooke Triplet with the intermediate merit function. Flint glasses down and to the left on the glass line will yield lenses with smaller airspaces; flints up and to the right will yield larger airspaces. Adjust the apertures to give roughly the required amount of vignetting. For each of the combinations, tabulate the value of the merit function and look at the layout and ray fan plot. The best glass pair will show a practical layout and have the lowest value of the merit function.

In the present Cooke Triplet example with the two crown elements made of Schott LaFN21 (n_d of 1.788, V_d of 47.5), the matching glass for the flint element is found to be, not SF15 (n_d of 1.699, V_d of 30.1) as was first guessed, but Schott SF53 (n_d of 1.728, V_d of 28.7). Both LaFN21 and SF53 are among Schott's preferred glass types.

B.3.4 Flattening the Field

When choosing glasses, it is important to consider the Petzval sum. Refer again to the discussion of Petzval sum in Chapter A.9. Recall that the Petzval sum gives the curvature of the Petzval surface, and that (when only considering astigmatism and field curvature) the Petzval surface is the best image surface when astigmatism is zero.

Thus, for a lens with little astigmatism, the Petzval sum must be made small to flatten the field. However, the sum need not be exactly zero because leaving in a small amount of Petzval curvature allows field-dependent defocus to be added to the off-axis aberration cancelling mix. The important thing is that the Petzval sum must be controllable during optimization.

For thin lens elements, the contribution to the Petzval sum by a given element goes directly as element power and inversely as element index of refraction. In a multi-element lens with an overall positive focal length, the elements with positive power necessarily predominate. Thus the Petzval sum will naturally tend to be sizable and negative, thereby giving an inward curving field (image surface concave to the light).

There are in general two ways to reduce the Petzval sum to flatten the field. They are: (1) glass selection and (2) axial separation of positive and negative optical powers. In practice, both ways are usually used together. As was mentioned in the previous section, the first way, glass selection, requires that the two positive elements of a Cooke Triplet be made of higher-index glass to give decreased negative Petzval contributions, and the negative element be made of lower-index glass to give an increased positive contribution. The second way, separation of powers, requires that the positive and negative elements be separated in a manner that causes the power of the negative element to be increased relative to the powers of the positive elements. The relatively larger negative power then gives a relatively larger positive Petzval contribution that reduces the Petzval sum.

To visualize how the second method works to flatten the field, examine the path of the upper marginal ray (for the on-axis object) as it passes through the optimized Cooke Triplet in Figure B.3.1.1. Note that the height of the ray is less on the middle negative element than on the front positive element, and consequently the ray slope is negative (downward) in the intervening front airspace. If the front airspace is made larger, and assuming the ray slope is roughly unchanged, then the height of the marginal ray on the middle element is reduced. But this reduced ray height requires that the middle element be given greater power (stronger curvatures) to bend the marginal ray by the angle necessary to give the required positive (upward) ray slope in the rear airspace. This use of airspaces is how the relative power of the negative element of a Cooke Triplet is increased to reduce the Petzval sum. The effect is greater as the airspaces are increased and the lens is stretched out.

Note that this reasoning applies to other lens types too. It even applies to lenses having thick meniscus elements. With a thick meniscus, there is again an axial separation of positive and negative powers. Now, however, the separation is between two surfaces on the same element, rather than between two different elements. Instead of an airspace, it is now a glass-space. Flattening the field with thick meniscus elements is called the thick-meniscus principle.

B.3.5 Vignetting

Like the vast majority of camera lenses, this Cooke Triplet example is to have mechanical vignetting of the off-axis pupils. Recall that mechanical vignetting is caused by undersized clear apertures on surfaces other than the stop surface, and these apertures selectively clip off-axis beams. Mechanical vignetting is useful for two reasons. First, the smaller lens elements reduce size, weight, and cost. Second and more fundamental, vignetting allows a better optical solution.

Most camera lenses of at least moderate speed and field coverage suffer from secondary and higher-order aberrations, both chromatic and monochromatic. Three prominent examples of secondary aberrations are secondary longitudinal color, secondary lateral color, and spherochromatism (chromatic variation of spherical aberration). Higher-order aberrations include the fifth-order, seventh-order, etc. counterparts of the third-order Seidel monochromatic aberrations. There are also aberrations that have no third-order form and begin with fifth- or higher-order, such as oblique spherical aberration, a fifth-order aberration. These secondary and higher-order aberrations are very resistant to control during optimization because they are usually a function of the basic optical configuration, not its specific implementation. For example, the Dagor lens just inherently has lots of on-axis zonal spherical, the result of lots of third-order spherical imperfectly balancing lots of fifth-order spherical. Similarly, the Double-Gauss lens has lots of off-axis oblique spherical.

For a lens with resistant on-axis aberrations, overall maximum system speed must be restricted. However, for resistant off-axis aberrations, system speed may need to be reduced only off-axis. To do this, you effectively stop down the lens only off-axis by using mechanical vignetting. In other words, to suppress resistant off-axis aberrations, it is often more effective to use undersized apertures to simply vignette away some of the worst offending rays rather than try to control them through optimization.

This may sound crude, but actually it is elegant when properly done. Mechanical vignetting allows you to concentrate the system's always limited degrees of freedom on reducing the remaining aberrations. The result is a much sharper lens with only a mild falloff in image illumination (irradiance), mostly in the corners. Compare the layouts in Figures B.3.1.1 and B.3.1.2. The first lens has vignetting (for simplification, the second and third fields have been omitted). The second lens has no vignetting (with all four fields drawn).

Conceptually, there are two different ways to handle mechanical vignetting when designing a lens. Both are available in ZEMAX. For this reason, and because ZEMAX happens to be the program the author uses, some of the details here apply specifically to ZEMAX, although the concepts are generally applicable.

The first way to handle vignetting uses real or hard apertures on lens surfaces

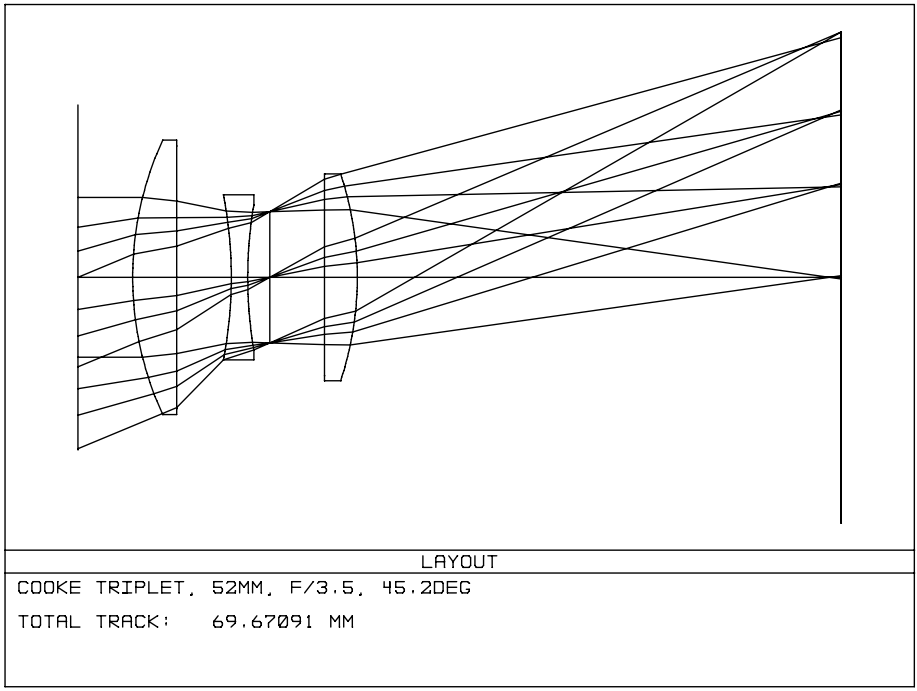

Figure B.3.1.2

to block and delete the vignetted portion of the off-axis rays. The second way uses vignetting factors or vignetting coefficients to reshape the off-axis beams to match the restricted vignetted pupil, thereby allowing all of the off-axis rays to pass through the lens to the image.

Each of these two methods has its advantages and disadvantages. The use of hard apertures is more realistic and can accommodate unusually shaped pupils and obscurations. But the use of hard apertures requires an optimization method that is less efficient and takes more computer time. The use of vignetting factors involves approximations to the actual situation and may introduce significant errors. But if vignetting factors are used (and they can be for most systems), then the computations are much faster, and finding the solution during optimization is more direct.

To illustrate both ways of handling vignetting, the present chapter uses hard apertures, and the following chapter uses vignetting factors.

In the present chapter, to construct a default merit function that includes vignetting, the entrance pupil is illuminated by simple grids of rays (the rectangular array option in ZEMAX). When projected onto the stop surface, the rectangular grids are actually square. Rays that are blocked by hard vignetting apertures are deleted from the ray sets. The same is true for central obscurations, although none

are present here. Only the rays that reach the image surface are included in the construction of the operands in the default merit function. This is a very general and physically realistic approach that is applicable to any optical system.

For many lens configurations, including the Cooke Triplet, only hard apertures on the front and rear surfaces need be considered when adjusting vignetting. These are the two surfaces most distant from the stop, and they are ideally placed for defining beam clipping. All other surfaces (except the stop) are made large enough to not clip rays that can pass through the two defining surfaces.

Exceptions to this approach are lenses having surfaces located large distances from the stop; that is, where system axial length on one or both sides of the stop is considerably longer than the entrance pupil diameter. Three prominent examples are true telephoto lenses, retrofocus type wide-angle lenses, and zoom lenses. Here, the transverse location (footprint) of off-axis beams on surfaces far from the stop can shift by much more than the beam diameter. For gradual mechanical vignetting in these lenses, the defining apertures must be closer to the stop.

When selecting vignetting apertures, try to clip similar amounts off the top and bottom of the extreme off-axis beam. This maintains as much symmetry as possible. However, this rule is neither precise nor rigid, and it can be bent if one side of the pupil has worse aberrations than the other side. Use layouts and ray fan plots to determine the relative top and bottom clipping. Use the geometrical throughput option in your program to precisely calculate the fraction of unvignetted rays passing through the stop surface as a function of off-axis distance or field angle. Pay special attention to relative throughput at the edge of the field, the worst case. Of course, the defining apertures must not clip the on-axis beam; the on-axis beam must be wholly defined by the stop aperture.

For the Cooke Triplet and many other lenses, a good approach is to make the defining front and rear apertures just a little bigger than the on-axis beam diameter, as illustrated by the lens in Figure B.3.1.1. With these apertures and proper airspaces, mechanical vignetting begins about a third of the way out toward the edge of the field and increases smoothly with field angle.

For most camera lenses, a relative geometrical transmission by the vignetted off-axis pupil of about 50% or slightly less at the edge of the field is scarcely noticeable with most films and other image detectors. In fact, this amount of vignetting is quite conservative; many excellent camera lenses have much more light falloff when used wide open. Therefore, when the Cooke Triplet is wide open at *f*/3.5, relative throughput of about 50% at the edge of the field is adopted here for the allowed amount of vignetting.

Note the convention: 60% vignetting means 40% throughput. Note too that as a lens is stopped down, the apparent mechanical vignetting decreases and image illumination (irradiance) becomes more uniform.

B.3.6 Starting Design and Early Optimizations

The optimization procedure outlined in Chapter A.15 has been adopted for designing this Cooke Triplet example.

When deriving a rough starting design, you first select the starting glasses (as described above). The next thing is to make guesses at the initial values of the system parameters; that is, the six curvatures, the two airspaces, and the three glass thicknesses. To automatically reduce the three transverse aberrations (lateral color, coma, and distortion), try to make the system as symmetrical about the stop as possible. Of course, perfect symmetry is impossible because the object is at infinity and the stop is not exactly at the middle element.

Initially, make the curvatures on the outer surfaces of the two positive elements equal with opposite signs. Make the curvatures on the inner surfaces of the two positive elements equal with opposite signs. And make the two curvatures on the middle negative element equal with opposite signs. The easy way to create this symmetry and maintain it during early optimizations is to use three curvature pickup solves to make the last three surface curvatures equal to the first three surface curvatures in reverse order and with opposite signs.

Because the stop is located in the rear airspace, better symmetry can be initially achieved by making the rear airspace (glass-to-glass) a bit larger than the front airspace. The easy way to do this is to use a thickness pickup solve to make the space between the stop and rear element equal to the space between the front and middle elements.

The three elements should be thin but realistic and easy to fabricate. Make the two positive elements thick enough to avoid tiny or negative edge thicknesses. Make the negative element thick enough to avoid a delicate center. The usual procedure is to manually select the glass center thicknesses and then to freeze or fix them; that is, they are kept constant during optimization. If a glass thickness becomes inappropriate as the design evolves, change it by hand and reoptimize. In addition, remember that this lens is physically quite small. Practical edges and centers may look deceptively thick when compared to the element diameters. A life-size layout can be very valuable in giving the designer a more intuitive awareness of the true sizes involved. In fact, at some time during the design of any lens, a life-size layout should be made.

To locate the image surface at the paraxial focus of the reference wavelength, proceed as in earlier chapters. Use a marginal ray paraxial height solve on the thickness following the last lens surface to determine the paraxial focal distance (paraxial BFL). Place a dummy plane surface at this distance to represent the paraxial focal plane. The actual image surface is a plane that immediately follows the paraxial focal plane. The two surfaces, at least initially, are given a zero separation. This general procedure is good technique and retains the option of adding paraxial defocus to the aberration balance during optimization. However,

this option is not always used. In particular, for both examples in this chapter, the image surface is kept at the paraxial focus; that is, no paraxial defocus is used.

Finally, because only hard apertures are to be allowed for controlling vignetting in this example, it is recommended that deliberate mechanical vignetting not be used at all in this early optimization stage of the Cooke Triplet. Vignetting can be introduced in the intermediate optimization stage. Note that this approach works for this *f*/3.5 lens, but may not work as well for a faster lens, such as the *f*/2 Double-Gauss lens in the next chapter.

Based on the above suggestions, the layout of one possible starting lens is illustrated in Figure B.3.1.2. This lens was derived by selecting the glasses and then tinkering with the curvatures and thicknesses until the layout looked about right (similar to published drawings). To simplify the guesswork, make the inner surfaces of the positive elements initially flat. Fortunately, the exact starting configuration is not too critical.

Note that because of the pickups, this starting lens has only four *independent* degrees of freedom: the first three curvatures and the first airspace. These are enough for now, but not enough to address all the basic aberrations.

The merit function for the early optimizations contains operands to correct focal length to 52 mm, prevent the airspaces from becoming too large or too small, correct paraxial longitudinal color for the two extreme wavelengths, and, using a default merit function, shrink polychromatic spots across the field. Correcting paraxial longitudinal color controls element powers and at this stage is very effective in shepherding the design in the right direction. A distortion operand is not included, but symmetry should keep distortion in check.

The early merit function is given in Listing B.3.1.1. To use the simplest allowable default merit function, some fields and wavelengths are weighted zero; this deletes the corresponding operands during the default merit function construction. Thus, the four fields are weighted 1 0 1 1 (in order from center to edge), and the five wavelengths are weighted 1 0 1 0 1 (in order from short to long). Because no beam clipping is used here to produce vignetting, a ray array based on the Gaussian quadrature algorithm is allowed and adopted (see Chapter B.4 for more on Gaussian quadrature).

After optimizing, look at the layout. This can be very revealing about how your glass choices affect the design. If your choice of matching flint glass gives a dispersion difference that is too large or too small, then the airspaces will be correspondingly too large or too small. If so, change the flint glass and reoptimize. The layout is your guide at this early optimization stage.

B.3.7 Intermediate Optimizations

You now have a good early design that is suitable for intermediate optimization. There are many ways to control aberrations. These methods are functions

Merit Function Listing

File : C:LENS311.ZMX
Title: COOKE TRIPLET, 52MM, F/3.5, 45.2DEG

Merit Function Value: 3.63793459E-002

Num	Type	Int1	Int2	Hx	Hy	Px	Py	Target	Weight	Value	% Cont
1	EFFL		3					5.20000E+001	1	5.20003E+001	0.000
2	BLNK										
3	BLNK										
4	MXCA	2	7					1.00000E+001	1	1.00000E+001	0.000
5	MNCA	2	7					1.00000E-001	1	1.00000E-001	0.000
6	MNEA	2	7					1.00000E-001	1	1.00000E-001	0.000
7	BLNK										
8	BLNK										
9	AXCL							0.00000E+000	10	-6.82493E-004	0.023
10	BLNK										
11	BLNK										
12	DMFS										
13	TRAR		1	0.0000	0.0000	0.4597	0.0000	0.00000E+000	0.07854	1.03524E-003	0.000
14	TRAR		1	0.0000	0.0000	0.8881	0.0000	0.00000E+000	0.07854	1.28006E-002	0.063
15	TRAR		3	0.0000	0.0000	0.4597	0.0000	0.00000E+000	0.07854	6.76146E-003	0.018
16	TRAR		3	0.0000	0.0000	0.8881	0.0000	0.00000E+000	0.07854	3.43827E-002	0.455
17	TRAR		5	0.0000	0.0000	0.4597	0.0000	0.00000E+000	0.07854	3.58840E-003	0.005
18	TRAR		5	0.0000	0.0000	0.8881	0.0000	0.00000E+000	0.07854	3.32670E-002	0.426
19	TRAR		1	0.0000	0.6991	0.2298	0.3981	0.00000E+000	0.02618	8.50000E-002	0.927
20	TRAR		1	0.0000	0.6991	0.4440	0.7691	0.00000E+000	0.02618	2.08535E-001	5.581
21	TRAR		1	0.0000	0.6991	0.4597	0.0000	0.00000E+000	0.02618	5.42000E-002	0.377
22	TRAR		1	0.0000	0.6991	0.8881	0.0000	0.00000E+000	0.02618	1.05953E-001	1.441
23	TRAR		1	0.0000	0.6991	0.2298	-0.3981	0.00000E+000	0.02618	2.04915E-002	0.054
24	TRAR		1	0.0000	0.6991	0.4440	-0.7691	0.00000E+000	0.02618	7.26274E-002	0.677
25	TRAR		3	0.0000	0.6991	0.2298	0.3981	0.00000E+000	0.02618	7.37596E-002	0.698
26	TRAR		3	0.0000	0.6991	0.4440	0.7691	0.00000E+000	0.02618	2.10582E-001	5.691
27	TRAR		3	0.0000	0.6991	0.4597	0.0000	0.00000E+000	0.02618	5.32878E-002	0.364
28	TRAR		3	0.0000	0.6991	0.8881	0.0000	0.00000E+000	0.02618	1.18142E-001	1.791
29	TRAR		3	0.0000	0.6991	0.2298	-0.3981	0.00000E+000	0.02618	2.04063E-002	0.053
30	TRAR		3	0.0000	0.6991	0.4440	-0.7691	0.00000E+000	0.02618	3.12326E-002	0.125
31	TRAR		5	0.0000	0.6991	0.2298	0.3981	0.00000E+000	0.02618	6.28696E-002	0.507
32	TRAR		5	0.0000	0.6991	0.4440	0.7691	0.00000E+000	0.02618	2.00040E-001	5.136
33	TRAR		5	0.0000	0.6991	0.4597	0.0000	0.00000E+000	0.02618	4.95950E-002	0.316
34	TRAR		5	0.0000	0.6991	0.8881	0.0000	0.00000E+000	0.02618	1.15423E-001	1.710
35	TRAR		5	0.0000	0.6991	0.2298	-0.3981	0.00000E+000	0.02618	2.41034E-002	0.075
36	TRAR		5	0.0000	0.6991	0.4440	-0.7691	0.00000E+000	0.02618	2.43297E-002	0.076
37	TRAR		1	0.0000	1.0000	0.2298	0.3981	0.00000E+000	0.02618	1.26323E-001	2.048
38	TRAR		1	0.0000	1.0000	0.4440	0.7691	0.00000E+000	0.02618	3.24527E-001	13.516
39	TRAR		1	0.0000	1.0000	0.4597	0.0000	0.00000E+000	0.02618	8.62986E-002	0.956
40	TRAR		1	0.0000	1.0000	0.8881	0.0000	0.00000E+000	0.02618	1.68672E-001	3.651
41	TRAR		1	0.0000	1.0000	0.2298	-0.3981	0.00000E+000	0.02618	6.70936E-002	0.578
42	TRAR		1	0.0000	1.0000	0.4440	-0.7691	0.00000E+000	0.02618	2.56002E-001	8.411
43	TRAR		3	0.0000	1.0000	0.2298	0.3981	0.00000E+000	0.02618	1.05619E-001	1.432
44	TRAR		3	0.0000	1.0000	0.4440	0.7691	0.00000E+000	0.02618	3.16643E-001	12.867
45	TRAR		3	0.0000	1.0000	0.4597	0.0000	0.00000E+000	0.02618	7.94419E-002	0.810
46	TRAR		3	0.0000	1.0000	0.8881	0.0000	0.00000E+000	0.02618	1.69222E-001	3.675
47	TRAR		3	0.0000	1.0000	0.2298	-0.3981	0.00000E+000	0.02618	3.34562E-002	0.144
48	TRAR		3	0.0000	1.0000	0.4440	-0.7691	0.00000E+000	0.02618	1.90654E-001	4.665
49	TRAR		5	0.0000	1.0000	0.2298	0.3981	0.00000E+000	0.02618	9.05470E-002	1.052
50	TRAR		5	0.0000	1.0000	0.4440	0.7691	0.00000E+000	0.02618	3.00899E-001	11.620
51	TRAR		5	0.0000	1.0000	0.4597	0.0000	0.00000E+000	0.02618	7.45595E-002	0.713
52	TRAR		5	0.0000	1.0000	0.8881	0.0000	0.00000E+000	0.02618	1.63310E-001	3.423
53	TRAR		5	0.0000	1.0000	0.2298	-0.3981	0.00000E+000	0.02618	2.42043E-002	0.075
54	TRAR		5	0.0000	1.0000	0.4440	-0.7691	0.00000E+000	0.02618	1.71502E-001	3.775

Listing B.3.1.1

of both the preferences of the designer and the features in his software. What follows is an approach that the author finds to be effective for many types of optical systems. The details are specific to the present Cooke Triplet, but the ideas are generally applicable.

As described in Chapter A.15, intermediate optimization is a combination monochromatic-polychromatic procedure. The monochromatic aberrations for a central wavelength and the chromatic aberrations for the extreme (or two widely spaced) wavelengths are controlled or corrected. For the intermediate optimizations of a Cooke Triplet, the pickups are removed and the six curvatures and two airspaces are all made independent variables. The height solve is retained to keep the image surface at the paraxial focus.

Now during the intermediate optimizations is also the time to add deliberate mechanical vignetting to the Cooke Triplet. The techniques required are discussed in an earlier section.

When constructing the intermediate merit function, select or define five special optimization operands such as those described in Chapter A.13 and Listing A.13.1. The first operand continues to correct focal length to 52 mm (here and subsequently, you can alternatively use an angle solve on the rear lens surface to control focal ratio). The second operand corrects longitudinal color to zero for the 0.8 pupil zone. The third operand corrects lateral color to zero at the edge of the field. The fourth operand corrects spherical aberration to zero on the paraxial focal plane and for the 0.9 pupil zone. The fifth operand corrects distortion to zero at the edge of the field. To correct these operands close to their targets, use relatively heavy weights or Lagrange multipliers.

Note in Listing A.13.1 that wavelengths are specified by the identifying numbers in the Int2 column and that the lens there uses only three wavelengths. However, the present lens uses five wavelengths. Thus, the special chromatic operands must now use wavelengths one and five. And the special monochromatic operands must now use wavelength three, the reference wavelength.

The only aberrations that remain to be controlled are all off-axis monochromatic aberrations. They are: coma, astigmatism, field curvature, and any number of higher-order monochromatic aberrations. These aberrations plus spherical (which is also present off-axis) interact in a complicated way. To control these aberrations during optimization, the most general and fail-safe approach is to shrink spot sizes by appending the appropriate default merit function to the special operands. Because the on-axis field is being corrected separately with special operands, turn off the axial field when constructing the default merit function and shrink only the off-axis spots. To do this, weight the on-axis field zero and weight the remaining fields equally (at least for now). The four field weights become 0 1 1 1. Similarly, to shrink only monochromatic spots for the reference wavelength, weight the five wavelengths 0 0 1 0 0.

The complete intermediate merit function for the Cooke Triplet is given in Listing B.3.1.2. To shorten the listing, the fields have actually been weighted 0 0 1 1.

Note that there is a variation to this approach that could have been used. Instead of controlling spherical aberration with a special operand, you can shrink the monochromatic on-axis spot too. To do this, omit the special spherical operand (to avoid controlling the same aberration twice), and construct the default merit function with field weights such as 5 1 1 1. The relatively heavy weight on-axis is required because spot size there is relatively small (no off-axis aberrations). The heavy weight ensures that the damped least-squares routine pays enough attention.

Note that different optical design programs may handle weights differently. Therefore, it is risky to recommend specific weights for controlling the relative emphasis of various field positions and wavelengths during optimization. This is especially true for nonuniform weights. Thus, the weights offered here are given

Merit Function Listing

File : C:LENS312B.ZMX
Title: COOKE TRIPLET, 52MM, F/3.5, 45.2DEG

Merit Function Value: 1.92724453E-004

Num	Type	Int1	Int2	Hx	Hy	Px	Py	Target	Weight	Value	% Cont
1	EFFL		3					5.20000E+001	100	5.20000E+001	0.000
2	BLNK										
3	BLNK										
4	TTHI	3	3					0.00000E+000	0	4.73834E+000	0.000
5	TTHI	5	6					0.00000E+000	0	6.45093E+000	0.000
6	DIFF	5	4					0.00000E+000	0	1.71259E+000	0.000
7	OPGT	6						1.50000E+000	100	1.50000E+000	0.000
8	BLNK										
9	BLNK										
10	AXCL							0.00000E+000	0	1.12374E-001	0.000
11	REAY	10	1	0.0000	0.0000	0.0000	0.8000	0.00000E+000	0	2.36923E-003	0.000
12	REAY	10	5	0.0000	0.0000	0.0000	0.8000	0.00000E+000	0	2.37042E-003	0.000
13	DIFF	11	12					0.00000E+000	10000	-1.19209E-006	0.001
14	BLNK										
15	BLNK										
16	LACL							0.00000E+000	0	1.39704E-002	0.000
17	REAY	10	1	0.0000	1.0000	0.0000	0.0000	0.00000E+000	0	2.16434E+001	0.000
18	REAY	10	5	0.0000	1.0000	0.0000	0.0000	0.00000E+000	0	2.16434E+001	0.000
19	DIFF	17	18					0.00000E+000	10000	-1.81699E-007	0.000
20	BLNK										
21	BLNK										
22	SPHA	0	3					0.00000E+000	0	2.64913E+000	0.000
23	REAY	9	3	0.0000	0.0000	0.0000	0.9000	0.00000E+000	10000	1.01362E-006	0.001
24	BLNK										
25	BLNK										
26	DIST	0	3					0.00000E+000	1000	5.36819E-008	0.000
27	BLNK										
28	BLNK										
29	DMFS										
30	TRAR		3	0.0000	0.6991	0.1000	-0.5000	0.00000E+000	0.1	6.12221E-003	0.323
31	TRAR		3	0.0000	0.6991	0.1000	-0.3000	0.00000E+000	0.1	4.34227E-003	0.163
32	TRAR		3	0.0000	0.6991	0.1000	-0.1000	0.00000E+000	0.1	4.43055E-003	0.169
33	TRAR		3	0.0000	0.6991	0.1000	0.1000	0.00000E+000	0.1	4.43263E-003	0.170
34	TRAR		3	0.0000	0.6991	0.1000	0.3000	0.00000E+000	0.1	4.66716E-003	0.188
35	TRAR		3	0.0000	0.6991	0.1000	0.5000	0.00000E+000	0.1	6.55600E-003	0.371
36	TRAR		3	0.0000	0.6991	0.1000	0.7000	0.00000E+000	0.1	1.42184E-002	1.744
37	TRAR		3	0.0000	0.6991	0.3000	-0.5000	0.00000E+000	0.1	1.26632E-002	1.384
38	TRAR		3	0.0000	0.6991	0.3000	-0.3000	0.00000E+000	0.1	1.28531E-002	1.425
39	TRAR		3	0.0000	0.6991	0.3000	-0.1000	0.00000E+000	0.1	1.34846E-002	1.569
40	TRAR		3	0.0000	0.6991	0.3000	0.1000	0.00000E+000	0.1	1.35945E-002	1.595
41	TRAR		3	0.0000	0.6991	0.3000	0.3000	0.00000E+000	0.1	1.35749E-002	1.590
42	TRAR		3	0.0000	0.6991	0.3000	0.5000	0.00000E+000	0.1	1.40286E-002	1.698
43	TRAR		3	0.0000	0.6991	0.3000	0.7000	0.00000E+000	0.1	1.91872E-002	3.176
44	TRAR		3	0.0000	0.6991	0.5000	-0.5000	0.00000E+000	0.1	1.90906E-002	3.144
45	TRAR		3	0.0000	0.6991	0.5000	-0.3000	0.00000E+000	0.1	2.01296E-002	3.496
46	TRAR		3	0.0000	0.6991	0.5000	-0.1000	0.00000E+000	0.1	2.20930E-002	4.211
47	TRAR		3	0.0000	0.6991	0.5000	0.1000	0.00000E+000	0.1	2.26538E-002	4.428
48	TRAR		3	0.0000	0.6991	0.5000	0.3000	0.00000E+000	0.1	2.22624E-002	4.276
49	TRAR		3	0.0000	0.6991	0.5000	0.5000	0.00000E+000	0.1	2.14883E-002	3.984
50	TRAR		3	0.0000	0.6991	0.5000	0.7000	0.00000E+000	0.1	2.62421E-002	5.942
51	TRAR		3	0.0000	0.6991	0.7000	-0.3000	0.00000E+000	0.1	2.24606E-002	4.353
52	TRAR		3	0.0000	0.6991	0.7000	-0.1000	0.00000E+000	0.1	2.62597E-002	5.950
53	TRAR		3	0.0000	0.6991	0.7000	0.1000	0.00000E+000	0.1	2.77273E-002	6.633
54	TRAR		3	0.0000	0.6991	0.7000	0.3000	0.00000E+000	0.1	2.65562E-002	6.085
55	TRAR		3	0.0000	0.6991	0.7000	0.5000	0.00000E+000	0.1	2.47190E-002	5.272
56	TRAR		3	0.0000	0.6991	0.9000	-0.1000	0.00000E+000	0.1	1.64515E-002	2.335
57	TRAR		3	0.0000	0.6991	0.9000	0.1000	0.00000E+000	0.1	1.77613E-002	2.722
58	TRAR		3	0.0000	0.6991	0.9000	0.3000	0.00000E+000	0.1	1.72447E-002	2.566
59	TRAR		3	0.0000	1.0000	0.1000	-0.3000	0.00000E+000	0.1	8.95928E-003	0.693
60	TRAR		3	0.0000	1.0000	0.1000	-0.1000	0.00000E+000	0.1	3.66083E-003	0.116
61	TRAR		3	0.0000	1.0000	0.1000	0.1000	0.00000E+000	0.1	3.79969E-003	0.125
62	TRAR		3	0.0000	1.0000	0.1000	0.3000	0.00000E+000	0.1	5.54200E-003	0.265
63	TRAR		3	0.0000	1.0000	0.1000	0.5000	0.00000E+000	0.1	2.92387E-003	0.074
64	TRAR		3	0.0000	1.0000	0.3000	-0.3000	0.00000E+000	0.1	4.43901E-003	0.170
65	TRAR		3	0.0000	1.0000	0.3000	-0.1000	0.00000E+000	0.1	3.89385E-003	0.131
66	TRAR		3	0.0000	1.0000	0.3000	0.1000	0.00000E+000	0.1	7.13892E-003	0.440
67	TRAR		3	0.0000	1.0000	0.3000	0.3000	0.00000E+000	0.1	7.82365E-003	0.528
68	TRAR		3	0.0000	1.0000	0.3000	0.5000	0.00000E+000	0.1	6.33420E-003	0.346
69	TRAR		3	0.0000	1.0000	0.5000	-0.1000	0.00000E+000	0.1	5.19208E-003	0.233
70	TRAR		3	0.0000	1.0000	0.5000	0.1000	0.00000E+000	0.1	9.23102E-003	0.735
71	TRAR		3	0.0000	1.0000	0.5000	0.3000	0.00000E+000	0.1	8.34579E-003	0.601
72	TRAR		3	0.0000	1.0000	0.5000	0.5000	0.00000E+000	0.1	9.90926E-003	0.847
73	TRAR		3	0.0000	1.0000	0.7000	-0.1000	0.00000E+000	0.1	1.65419E-002	2.361
74	TRAR		3	0.0000	1.0000	0.7000	0.1000	0.00000E+000	0.1	9.28791E-003	0.744
75	TRAR		3	0.0000	1.0000	0.7000	0.3000	0.00000E+000	0.1	9.97684E-004	0.009
76	TRAR		3	0.0000	1.0000	0.9000	0.1000	0.00000E+000	0.1	3.50863E-002	10.621

Listing B.3.1.2

with a caveat. The best advice to the lens designer is to experiment with weights until you get results that you like.

In the design of a Cooke Triplet, you will often find two possible solutions; that is, two different local minima of the merit function. The first solution has the larger airspace between the front and middle elements; the second solution has the larger airspace between the middle and rear elements. As mentioned earlier, better symmetry about the stop is achieved if the rear airspace is the larger one. This more symmetrical configuration causes the off-axis beams to be more centered about their chief rays, which is better when stopping down the lens. To shepherd the design in this direction, a constraint is added to the intermediate merit function that keeps the rear airspace (glass-to-glass) somewhat larger than the front airspace.

After optimizing with the airspace constraint, look at the merit function to see if it was invoked. It may have been unused. If it was used, try removing it (perhaps by setting its weight to zero) and optimize again. The lens will then find its own best airspaces. However, do not be surprised if the negative element ends up nearly in the middle between the two positive elements, or if you occasionally have to leave in the constraint.

After each optimization run, the system parameters (curvatures and airspaces) will have changed to a greater or lesser extent, thereby also changing the size and shape of the vignetted off-axis pupils. To accommodate these changes, rebuild the default merit function to update the set of unvignetted rays, and then reoptimize. Iterate as needed. In addition, the lens designer is also often required to manually readjust the diameters of the hard apertures to maintain the desired amount of vignetting. After any such change, again rebuild the default merit function and reoptimize.

The last step in the intermediate optimizations is finding the best flint glass type. To do this, repeat the intermediate optimization with several likely glass combinations. The process is described in an earlier section. The result for the present Cooke Triplet is that Schott SF53 flint glass (n_d of 1.728, V_d of 28.7) is the best match for Schott LaFN21 crown glass (n_d of 1.788, V_d of 47.5).

B.3.2 Final Optimizations Using Spot Size

The intermediate solution for the Cooke Triplet is actually quite close to the final solution. The final solution is a refinement, which is normally accomplished in two stages. The first stage shrinks polychromatic spots on the image surface. The second stage minimizes polychromatic OPD errors in the exit pupil. The designer then compares the two solutions and chooses the better one for the given application. If MTF is the image criterion, then the OPD solution is usually, but not always, preferable.

There are two ways to do the final spot optimization. The first way uses a

merit function that shrinks polychromatic spot sizes for all field positions and all wavelengths while continuing to correct distortion and focal length with special operands. Note that longitudinal and lateral color are not individually corrected; the polychromatic spot optimization includes the chromatic aberrations. Thus, when constructing the default merit function, weight the four fields equally; that is, 1 1 1 1, at least initially. Also weight the five wavelengths equally; that is, 1 1 1 1. As an alternative, you might do as just described plus still continue to exactly correct longitudinal color with a special operand to ensure a specific color curve.

The second way is very similar except that the on-axis aberrations (longitudinal color and spherical aberration) are corrected with special operands, and the default merit function shrinks polychromatic spots only off-axis. Again, distortion and focal length are specially corrected. When constructing the default merit function, the on-axis spot is turned off by weighting this field position zero; that is, field weights are 0 1 1 1 (at least initially). The polychromatic wavelength weights are again 1 1 1 1 1. In the present Cooke Triplet example, this second method has been adopted for constructing the merit function.

Listing B.3.1.3 gives the complete final merit function using spot size. An operand has also been included to control the relative airspaces, although it is not invoked during optimization. Field weights have been changed to 0 5 5 1 (see below). To make the figure of manageable size for printing, the default merit function is shown using 4x4 rectangular ray arrays; in reality, 10x10 or 20x20 ray arrays are used.

After optimizing, the size and shape of the vignetted off-axis pupil will have again changed. Again, rebuild the default merit function to match the new pupil and reoptimize.

As in the intermediate optimization stage, during the final optimizations, look at the layout, transverse ray fan plot, and spot diagram to monitor your solution. Repeat these tests frequently as your design continues to evolve. In addition, you may wish to look at the vignetting plot, the field curvature plot, the distortion plot, and the OPD ray fan plot. And, especially toward the end of these optimizations, the MTF plot is invaluable because MTF is your ultimate performance criterion. Except right at the end, you may wish to save computing time by using the geometrical MTF plot instead of the diffraction MTF plot; this shortcut is allowed because you are far from the diffraction limit.

By now in your design of a Cooke Triplet, it should have become apparent that the 100% field position tends to give better imagery than the 70% field position. This is not what you normally want. In a camera lens, the intermediate fields are normally more important than the edge of the field. Of course, there is less vignetting at intermediate fields, thereby allowing some of the more highly aberrated rays to get through. But a look at the tangential-sagittal field curvature plot, such as the left side of Figure B.3.1.5, reveals another problem. In a Cooke Triplet, there is a

Merit Function Listing

File : C:LENS313B.ZMX
Title: COOKE TRIPLET, 52MM, F/3.5, 45.2DEG

Merit Function Value: 5.16722085E-004

Num	Type	Int1	Int2	Hx	Hy	Px	Py	Target	Weight	Value	% Cont
1	EFFL		3					5.20000E+001	1000	5.20000E+001	0.000
2	BLNK										
3	BLNK										
4	TTHI	3	3					0.00000E+000	0	4.32187E+000	0.000
5	TTHI	5	6					0.00000E+000	0	6.85434E+000	0.000
6	DIFF	5	4					0.00000E+000	0	2.53247E+000	0.000
7	OPGT	6						1.50000E+000	1000	1.50000E+000	0.000
8	BLNK										
9	BLNK										
10	AXCL							0.00000E+000	0	1.11785E-001	0.000
11	REAY	10	1	0.0000	0.0000	0.0000	0.8000	0.00000E+000	0	2.26244E-003	0.000
12	REAY	10	5	0.0000	0.0000	0.0000	0.8000	0.00000E+000	0	2.33925E-003	0.000
13	DIFF	11	12					0.00000E+000	10000	-7.68052E-005	0.959
14	BLNK										
15	BLNK										
16	SPHA	0	3					0.00000E+000	0	2.69377E+000	0.000
17	REAY	9	3	0.0000	0.0000	0.0000	0.9000	0.00000E+000	10000	1.10586E-004	1.989
18	BLNK										
19	BLNK										
20	DIST	0	3					0.00000E+000	1000	2.01569E-006	0.000
21	BLNK										
22	BLNK										
23	DMFS										
24	TRAR		1	0.0000	0.3982	0.2500	-0.7500	0.00000E+000	0.5	1.13189E-002	1.042
25	TRAR		1	0.0000	0.3982	0.2500	-0.2500	0.00000E+000	0.5	6.13682E-003	0.306
26	TRAR		1	0.0000	0.3982	0.2500	0.2500	0.00000E+000	0.5	6.79766E-003	0.376
27	TRAR		1	0.0000	0.3982	0.2500	0.7500	0.00000E+000	0.5	4.29339E-003	0.150
28	TRAR		1	0.0000	0.3982	0.7500	-0.2500	0.00000E+000	0.5	8.61819E-003	0.604
29	TRAR		1	0.0000	0.3982	0.7500	0.2500	0.00000E+000	0.5	1.09141E-002	0.969
30	TRAR		2	0.0000	0.3982	0.2500	-0.7500	0.00000E+000	0.5	4.39938E-003	0.157
31	TRAR		2	0.0000	0.3982	0.2500	-0.2500	0.00000E+000	0.5	7.75161E-003	0.489
32	TRAR		2	0.0000	0.3982	0.2500	0.2500	0.00000E+000	0.5	7.13903E-003	0.414
33	TRAR		2	0.0000	0.3982	0.2500	0.7500	0.00000E+000	0.5	8.18535E-003	0.545
34	TRAR		2	0.0000	0.3982	0.7500	-0.2500	0.00000E+000	0.5	1.46952E-002	1.756
35	TRAR		2	0.0000	0.3982	0.7500	0.2500	0.00000E+000	0.5	1.75552E-002	2.506
36	TRAR		3	0.0000	0.3982	0.2500	-0.7500	0.00000E+000	0.5	4.13661E-003	0.139
37	TRAR		3	0.0000	0.3982	0.2500	-0.2500	0.00000E+000	0.5	6.83198E-003	0.380
38	TRAR		3	0.0000	0.3982	0.2500	0.2500	0.00000E+000	0.5	5.77825E-003	0.272
39	TRAR		3	0.0000	0.3982	0.2500	0.7500	0.00000E+000	0.5	7.22030E-003	0.424
40	TRAR		3	0.0000	0.3982	0.7500	-0.2500	0.00000E+000	0.5	1.48809E-002	1.801
41	TRAR		3	0.0000	0.3982	0.7500	0.2500	0.00000E+000	0.5	1.74078E-002	2.464
42	TRAR		4	0.0000	0.3982	0.2500	-0.7500	0.00000E+000	0.5	5.52951E-003	0.249
43	TRAR		4	0.0000	0.3982	0.2500	-0.2500	0.00000E+000	0.5	4.88180E-003	0.194
44	TRAR		4	0.0000	0.3982	0.2500	0.2500	0.00000E+000	0.5	4.11031E-003	0.137
45	TRAR		4	0.0000	0.3982	0.2500	0.7500	0.00000E+000	0.5	5.03739E-003	0.206
46	TRAR		4	0.0000	0.3982	0.7500	-0.2500	0.00000E+000	0.5	1.21386E-002	1.198
47	TRAR		4	0.0000	0.3982	0.7500	0.2500	0.00000E+000	0.5	1.44850E-002	1.706
48	TRAR		5	0.0000	0.3982	0.2500	-0.7500	0.00000E+000	0.5	9.21534E-003	0.691
49	TRAR		5	0.0000	0.3982	0.2500	-0.2500	0.00000E+000	0.5	3.01616E-003	0.074
50	TRAR		5	0.0000	0.3982	0.2500	0.2500	0.00000E+000	0.5	3.22798E-003	0.085
51	TRAR		5	0.0000	0.3982	0.2500	0.7500	0.00000E+000	0.5	5.54136E-003	0.250
52	TRAR		5	0.0000	0.3982	0.7500	-0.2500	0.00000E+000	0.5	8.23579E-003	0.552
53	TRAR		5	0.0000	0.3982	0.7500	0.2500	0.00000E+000	0.5	1.04533E-002	0.889
54	TRAR		1	0.0000	0.6991	0.2500	-0.2500	0.00000E+000	0.5	1.18736E-002	1.146
55	TRAR		1	0.0000	0.6991	0.2500	0.2500	0.00000E+000	0.5	1.22854E-002	1.227
56	TRAR		1	0.0000	0.6991	0.2500	0.7500	0.00000E+000	0.5	1.48341E-002	1.789
57	TRAR		1	0.0000	0.6991	0.7500	-0.2500	0.00000E+000	0.5	1.72910E-002	2.431
58	TRAR		1	0.0000	0.6991	0.7500	0.2500	0.00000E+000	0.5	2.11634E-002	3.642
59	TRAR		2	0.0000	0.6991	0.2500	-0.2500	0.00000E+000	0.5	1.34572E-002	1.473
60	TRAR		2	0.0000	0.6991	0.2500	0.2500	0.00000E+000	0.5	1.23649E-002	1.243
61	TRAR		2	0.0000	0.6991	0.2500	0.7500	0.00000E+000	0.5	1.53093E-002	1.906
62	TRAR		2	0.0000	0.6991	0.7500	-0.2500	0.00000E+000	0.5	2.26614E-002	4.176
63	TRAR		2	0.0000	0.6991	0.7500	0.2500	0.00000E+000	0.5	2.82597E-002	6.494
64	TRAR		3	0.0000	0.6991	0.2500	-0.2500	0.00000E+000	0.5	1.24155E-002	1.253
65	TRAR		3	0.0000	0.6991	0.2500	0.2500	0.00000E+000	0.5	1.12590E-002	1.031
66	TRAR		3	0.0000	0.6991	0.2500	0.7500	0.00000E+000	0.5	1.80932E-002	2.662
67	TRAR		3	0.0000	0.6991	0.7500	-0.2500	0.00000E+000	0.5	2.30272E-002	4.312
68	TRAR		3	0.0000	0.6991	0.7500	0.2500	0.00000E+000	0.5	2.85360E-002	6.622
69	TRAR		4	0.0000	0.6991	0.2500	-0.2500	0.00000E+000	0.5	1.05241E-002	0.901
70	TRAR		4	0.0000	0.6991	0.2500	0.2500	0.00000E+000	0.5	9.94036E-003	0.803
71	TRAR		4	0.0000	0.6991	0.2500	0.7500	0.00000E+000	0.5	2.20493E-002	3.953
72	TRAR		4	0.0000	0.6991	0.7500	-0.2500	0.00000E+000	0.5	2.09049E-002	3.554
73	TRAR		4	0.0000	0.6991	0.7500	0.2500	0.00000E+000	0.5	2.60342E-002	5.512
74	TRAR		5	0.0000	0.6991	0.2500	-0.2500	0.00000E+000	0.5	8.88009E-003	0.641
75	TRAR		5	0.0000	0.6991	0.2500	0.2500	0.00000E+000	0.5	8.85322E-003	0.637
76	TRAR		5	0.0000	0.6991	0.2500	0.7500	0.00000E+000	0.5	2.67318E-002	5.811
77	TRAR		5	0.0000	0.6991	0.7500	-0.2500	0.00000E+000	0.5	1.80876E-002	2.660
78	TRAR		5	0.0000	0.6991	0.7500	0.2500	0.00000E+000	0.5	2.24098E-002	4.084
79	TRAR		1	0.0000	1.0000	0.2500	-0.2500	0.00000E+000	0.1	3.54277E-002	2.041
80	TRAR		1	0.0000	1.0000	0.2500	0.2500	0.00000E+000	0.1	1.64360E-002	0.439
81	TRAR		1	0.0000	1.0000	0.7500	0.2500	0.00000E+000	0.1	1.29293E-002	0.272
82	TRAR		2	0.0000	1.0000	0.2500	-0.2500	0.00000E+000	0.1	2.87876E-002	1.348
83	TRAR		2	0.0000	1.0000	0.2500	0.2500	0.00000E+000	0.1	1.25153E-002	0.255
84	TRAR		2	0.0000	1.0000	0.7500	0.2500	0.00000E+000	0.1	4.61541E-003	0.035
85	TRAR		3	0.0000	1.0000	0.2500	-0.2500	0.00000E+000	0.1	2.09629E-002	0.715
86	TRAR		3	0.0000	1.0000	0.2500	0.2500	0.00000E+000	0.1	9.28730E-003	0.140
87	TRAR		3	0.0000	1.0000	0.7500	0.2500	0.00000E+000	0.1	4.84668E-003	0.038
88	TRAR		4	0.0000	1.0000	0.2500	-0.2500	0.00000E+000	0.1	1.32269E-002	0.285
89	TRAR		4	0.0000	1.0000	0.2500	0.2500	0.00000E+000	0.1	6.43729E-003	0.067
90	TRAR		4	0.0000	1.0000	0.7500	0.2500	0.00000E+000	0.1	8.04721E-003	0.105
91	TRAR		5	0.0000	1.0000	0.2500	-0.2500	0.00000E+000	0.1	5.90391E-003	0.057
92	TRAR		5	0.0000	1.0000	0.2500	0.2500	0.00000E+000	0.1	3.94329E-003	0.025
93	TRAR		5	0.0000	1.0000	0.7500	0.2500	0.00000E+000	0.1	1.22290E-002	0.243

Listing B.3.1.3

large difference between the tangential and sagittal curves at intermediate fields, but the curves cross near the field edge. Thus, at intermediate field zones you get a lot of astigmatism, but astigmatism goes to zero near the field edge.

This astigmatic behavior is the result of the interaction of relatively large amounts of third- and fifth-order astigmatism (seventh is negligible). The sum of the third- and fifth-orders is zero at the field angle where the curves cross. Unfortunately, at other field angles the sum may not be small. Third-order predominates inside the crossing, and fifth-order predominates outside the crossing. The problem is analogous to zonal spherical aberration, except that the effect is in the field, not the pupil. Significant residual field-zonal astigmatism is part of the inherent nature of a Cooke Triplet.

The use of high-index glasses generally reduces this astigmatism and is highly recommended. The only other thing you can do is tell the computer to change its priorities and emphasize the intermediate fields at the expense of the field edge; that is, you increase the relative weights on the two intermediate fields during optimization. This moves the field angle for zero astigmatism inward. Unfortunately, astigmatism increases very rapidly for field angles outside the tangential-sagittal crossing. You must therefore be very careful to avoid overdoing this brute force tactic. Also, the computer has other aberrations to worry about besides astigmatism, which is why the crossing initially fell so far out. A reasonable solution is obtained if the default part of the merit function is rebuilt with the field weights changed from 0 1 1 1 to 0 5 5 1 (while continuing to separately correct the on-axis field with special operands). The intermediate fields get better while the edge of the field gets worse.

This illustrates a recurrent situation in lens design. A given lens configuration has only a certain ability to control aberrations. If you take a previously optimized lens and reoptimize it to make one thing better, something else must get worse. There is an adage that says that the process of reoptimizing a lens is like squeezing on a water balloon. If you squeeze in one place, it pops out somewhere else.

Figure B.3.1.1 shows the layout of the Cooke Triplet as optimized by correcting focal length, distortion, and special on-axis operands; by shrinking polychromatic off-axis spots; and by emphasizing the intermediate fields. For increased clarity, the beams for only two fields have been drawn, the on-axis field and the extreme off-axis field. Note the mechanical vignetting of the off-axis beam by the front and rear outside lens surfaces. Note too that what appears to be the off-axis chief ray does not go through the center of the stop. Actually, the ray in question is not the chief ray, but is merely the middle ray of the ray bundle. The true chief ray always goes exactly through the center of the stop, by definition.

Figure B.3.1.3 is the vignetting diagram showing the fraction of unvignetted rays as a function of field angle. This plot confirms that vignetting is well-behaved and is about 50% at the edge of the field.

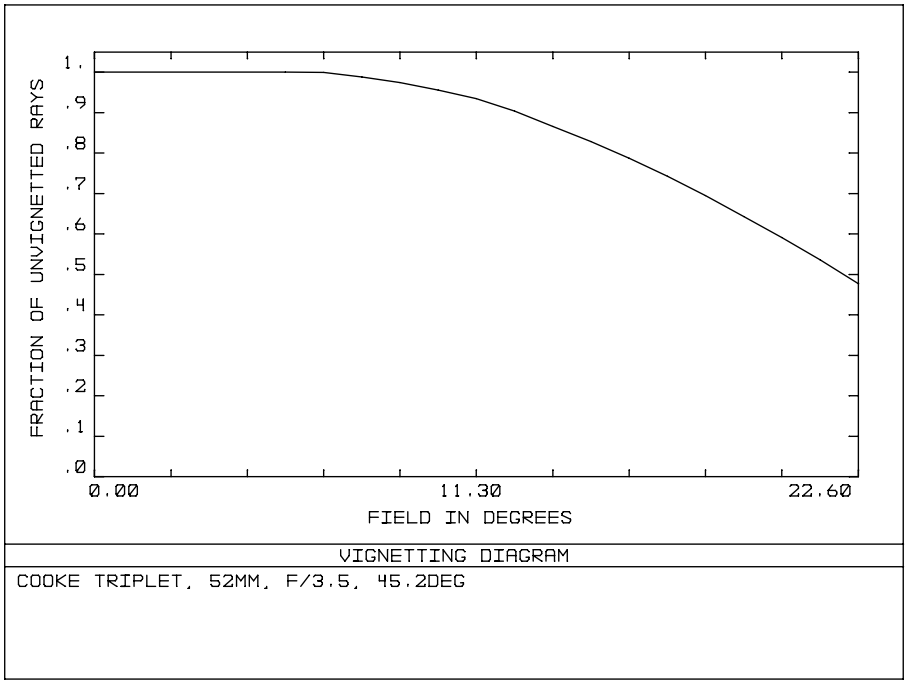

Figure B.3.1.3

Figure B.3.1.4 is the transverse ray fan plot. Note the well-behaved on-axis curves. For the three off-axis fields, note how the slopes of the tangential and sagittal curves are different at the origin, indicating astigmatism. Note too the oblique spherical aberration in the off-axis fields. Finally, note that the chromatic aberrations are relatively small compared to the monochromatic aberrations.

On the left side of Figure B.3.1.5 is the field curvature plot. Note the crossing of the tangential and sagittal curves near the field edge and the large astigmatic difference at intermediate field angles. On the right side of Figure B.3.1.5 is the percent distortion plot. Distortion has been corrected to zero at the field edge, but note the higher-order distortion residuals at intermediate field angles. These residuals are tiny and totally negligible for most purposes.

Figure B.3.1.6 is the polychromatic spot diagram. Note the different appearance of the spots. The spot for the 70% field is spread horizontally by tangential astigmatism, and the spot for the field edge is spread vertically by sagittal (radial) astigmatism. However, these images are not purely astigmatic because other aberrations are complicating the situation.

Figure B.3.1.7 is the matrix spot diagram. Note that the spots vary strongly with field but only moderately with wavelength.

Figure B.3.1.8 is the OPD ray fan plot. Note the scale: several waves. Clear-

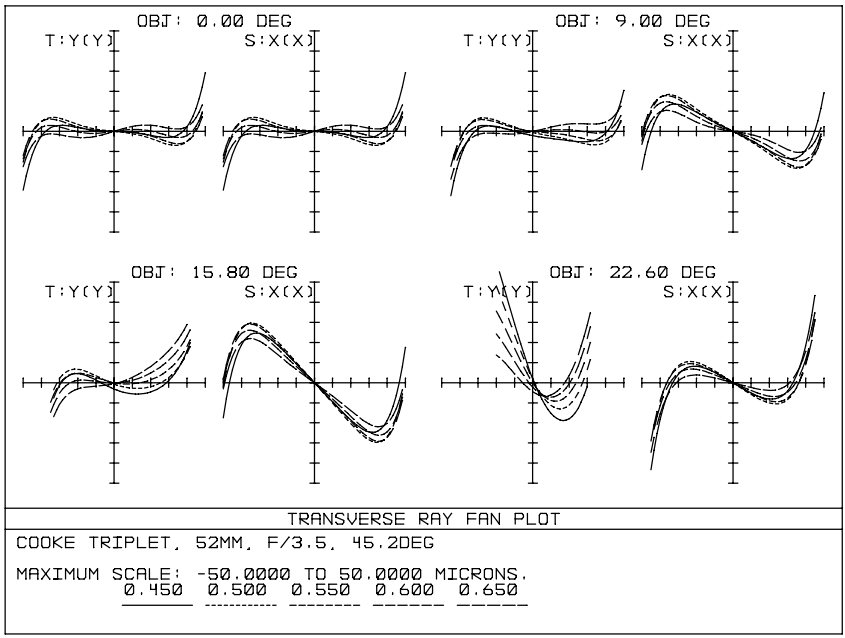

Figure B.3.1.4

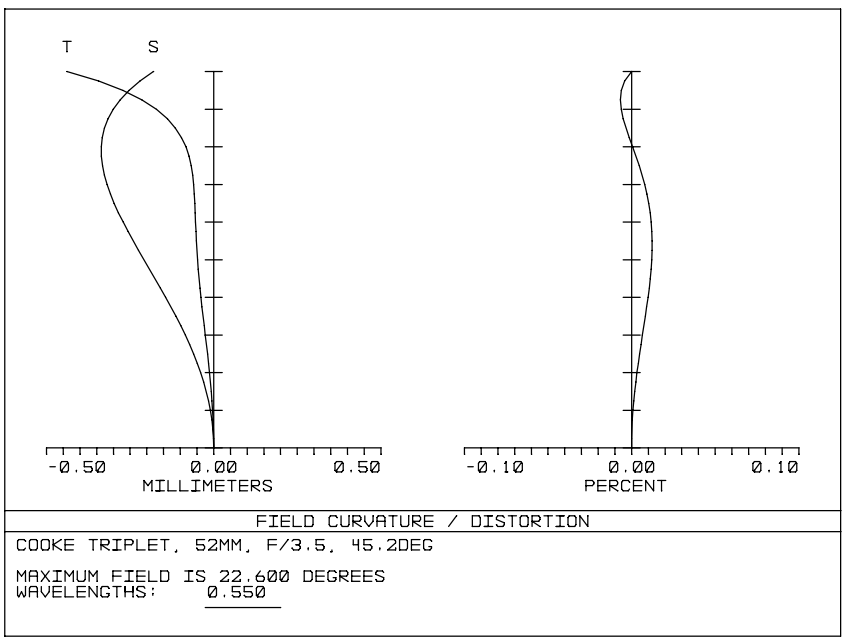

Figure B.3.1.5

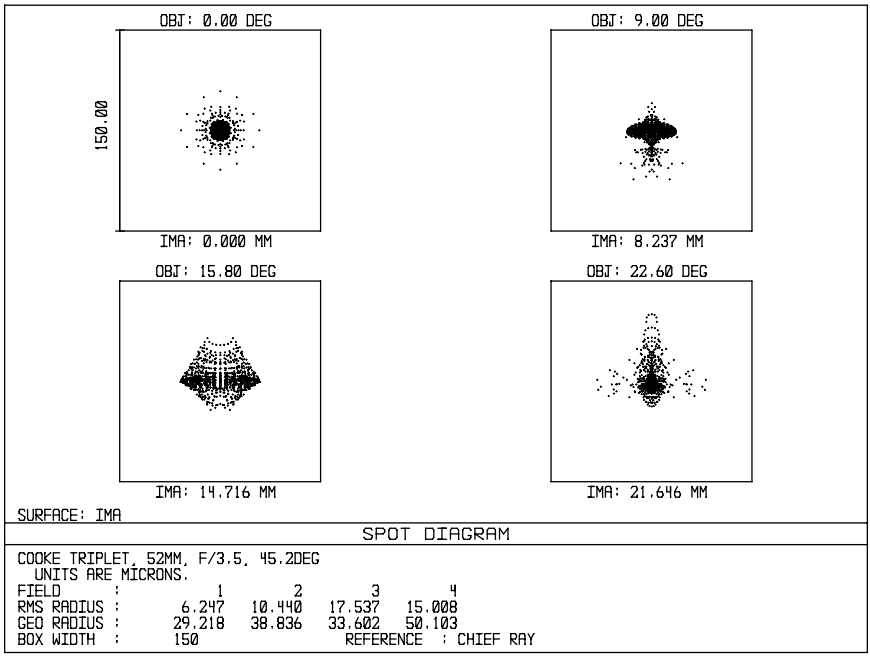

Figure B.3.1.6

ly, this lens is aberration limited, not diffraction limited. Even on-axis, this lens does not satisfy the Rayleigh quarter-wave rule. But this performance level is normal for this type of lens and is no cause for concern. At *f*/3.5 and for a wavelength of 0.55 μm, the diameter of the Airy disk is only 4.7 μm and the diffraction MTF cutoff is 520 cycles/mm. These values are much finer than most films can resolve. In fact, very few camera lenses are diffraction limited when used wide open, and most of these are slow, long-focus lenses.

Figure B.3.1.9 is the diffraction MTF plot. Even with increased weight on the intermediate fields during optimization, the sagittal MTF at the 70% field is very poor. Still heavier weights are not recommended; the spot size at the edge of the field would explode without much benefit to the intermediate fields. Note the spurious resolution. This artifact of the periodic nature of a pure spatial frequency is of no help for real images; modulations beyond the first zero must be ignored when evaluating lens performance.

Listing B.3.1.4 is the optical prescription for the spot size optimized Cooke Triplet. From this listing, you could build the lens. However, for a practical camera lens intended for use with films having a resolving capability in excess of 50 cycles/mm, this design for the Cooke Triplet is probably unacceptable, at least by modern standards based on MTF.

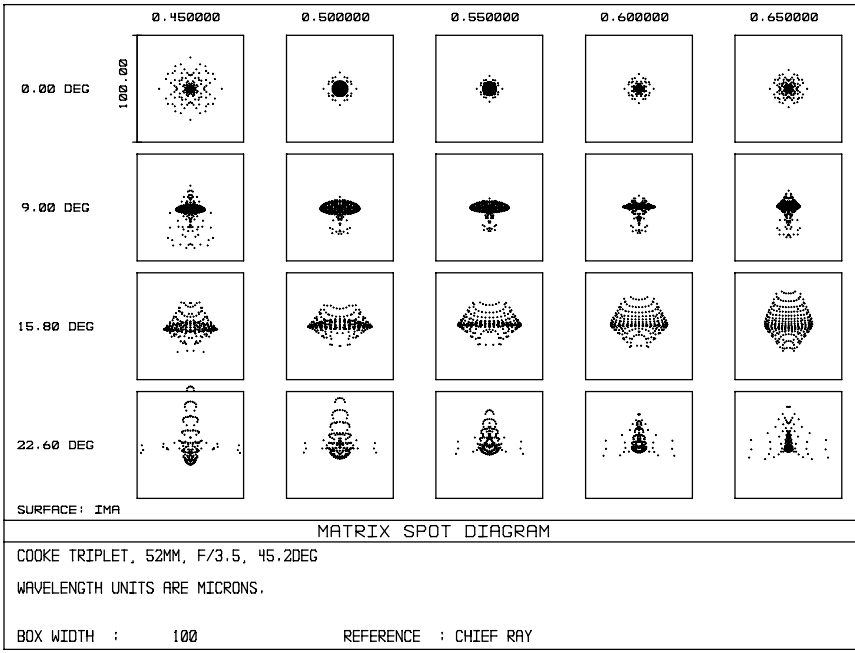

Figure B.3.1.7

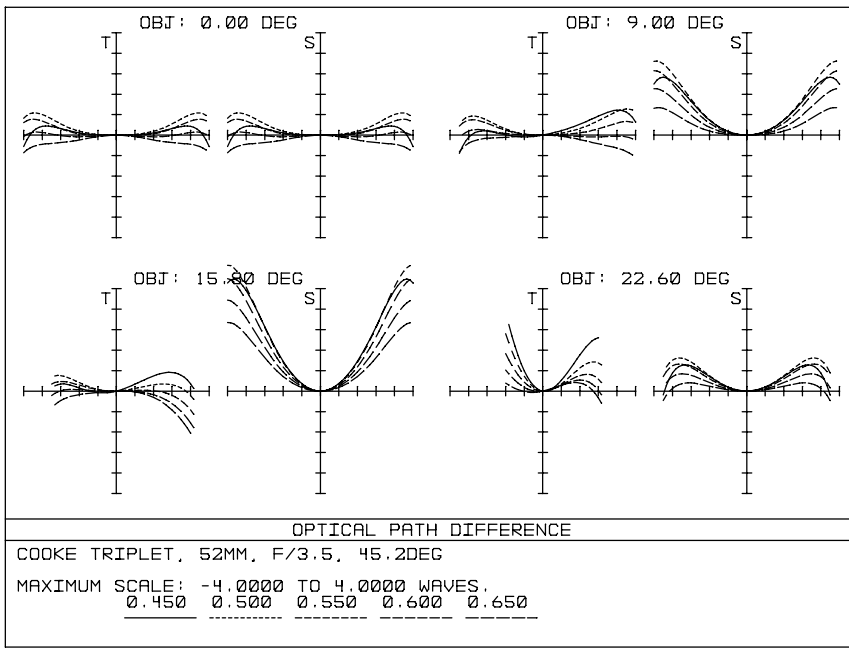

Figure B.3.1.8

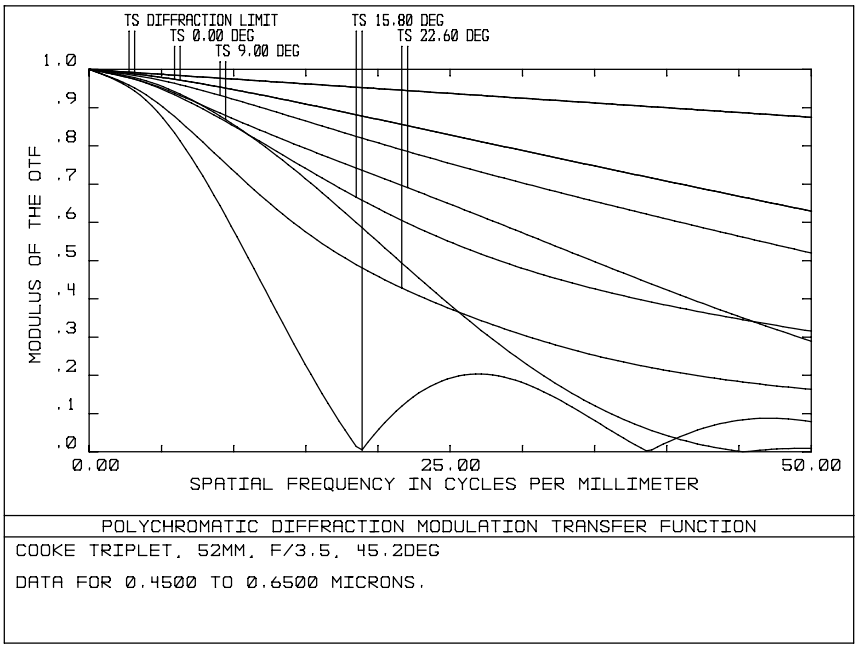

Figure B.3.1.9

B.3.2 Final Optimizations Using OPD Errors

For this Cooke Triplet example, there is not much more that you can do to improve image quality by shrinking spots. Because MTF is the criterion for image quality, a better approach may be to reduce wavefront OPD errors. Even though this lens is not near the diffraction limit, an OPD optimization may be beneficial. But bear in mind that if you optimize for minimum OPDs, then spot sizes may be small but they are no longer minimized. You cannot have it both ways. Remember the water balloon.

In the OPD optimization, all special optimization operands are removed from the merit function except those correcting or controlling distortion, focal length, and the relative airspace thicknesses. The bulk of the merit function is the default part that controls exit pupil OPDs for all fields and all wavelengths. The five wavelengths are again weighted 1 1 1 1 1. The four fields might be initially weighted 5 1 1 1. As suggested earlier, the on-axis field is more heavily weighted to ensure that the damped least-squares routine pays enough attention. The pupil is uniformly weighted with no extra emphasis on the center. No other prior assumptions are made. The goal is to do a polychromatic OPD optimization in a natural or realistic way (as it was called in Chapter A.15)

```
System/Prescription Data

File : C:LENS313B.ZMX
Title: COOKE TRIPLET, 52MM, F/3.5, 45.2DEG

GENERAL LENS DATA:

Surfaces         :          10
Stop             :           6
System Aperture :Entrance Pupil Diameter
Ray aiming       : On
 X Pupil shift   : 0
 Y Pupil shift   : 0
 Z Pupil shift   : 0
Apodization      :Uniform, factor =     0.000000
Eff. Focal Len. :           52 (in air)
Eff. Focal Len. :           52 (in image space)
Total Track      :       67.753
Image Space F/# :      3.49933
Para. Wrkng F/# :      3.49933
Working F/#      :      3.55795
Obj. Space N.A. :    7.43e-010
Stop Radius      :      5.73158
Parax. Ima. Hgt.:      21.6455
Parax. Mag.      :            0
Entr. Pup. Dia. :        14.86
Entr. Pup. Pos. :      19.9395
Exit Pupil Dia. :      14.1746
Exit Pupil Pos. :     -49.6015
Field Type       : Angle in degrees
Maximum Field    :         22.6
Primary Wave     :     0.550000
Lens Units       : Millimeters
Angular Mag.     :      1.04835

Fields           : 4
Field Type:  Angle in degrees
#       X-Value       Y-Value          Weight
1      0.000000      0.000000        0.000000
2      0.000000      9.000000        5.000000
3      0.000000     15.800000        5.000000
4      0.000000     22.600000        1.000000
```

Listing B.3.1.4

Listing B.3.2.1 is the complete final merit function for an OPD optimization. The field weights have been changed to 4 3 2 1 (see below). Again for practical reasons, 4x4 ray arrays are shown, although 10x10 or 20x20 arrays are actually used when optimizing. Note that the control on the relative airspace thicknesses is not invoked.

After optimizing with OPDs, the lens elements will have shifted by some amount relative to their positions for the minimum spot size solution. Thus, after the first OPD optimization, the vignetting will have changed and you must rebuild the default merit function and reoptimize. In addition, you may wish to fine tune the vignetting curve to give a specific throughput value at the edge of the field. This is done by slightly changing the vignetting apertures, again rebuilding the merit function, and again reoptimizing.

Next, do the usual layout, transverse ray fan plot, and spot diagram as sanity checks. Then do an OPD ray fan plot to check your OPD optimization. Finally, do the crucial MTF plot. As with a spot size optimization, an OPD optimization with uniform weights on the off-axis fields yields poorer performance for the intermediate fields than for the extreme field. The (partial) remedy once again is to increase the weights on the intermediate fields. Try different sets of weights, reoptimize for each set, and compare the MTF curves. Select the weights that give the best overall compromise. In the present case, field weights of 4 3 2 1 are found to work well.

Recall that in the present example, vignetting is handled during optimization

```
Vignetting Factors
#          VDX             VDY             VCX             VCY
1       0.000000        0.000000        0.000000        0.000000
2       0.000000        0.000000        0.000000        0.000000
3       0.000000        0.000000        0.000000        0.000000
4       0.000000        0.000000        0.000000        0.000000

Wavelengths     : 5
Units:  Microns
#          Value          Weight
1        0.450000        1.000000
2        0.500000        1.000000
3        0.550000        1.000000
4        0.600000        1.000000
5        0.650000        1.000000

SURFACE DATA SUMMARY:

Surf      Type          Radius       Thickness          Glass       Diameter        Conic
 OBJ   STANDARD       Infinity        Infinity                              0            0
   1   STANDARD       Infinity               7                       33.36006            0
   2   STANDARD       21.74267             3.5         LAFN21              17            0
   3   STANDARD       400.8834        4.321867                           17            0
   4   STANDARD      -43.54159             1.5           SF53              13            0
   5   STANDARD       20.87459               2                           12            0
 STO   STANDARD       Infinity        4.854339                       11.46317            0
   7   STANDARD       165.5048               3         LAFN21              15            0
   8   STANDARD       -30.5771        41.57679                           15            0
   9   STANDARD       Infinity               0                       43.61234            0
 IMA   STANDARD       Infinity               0                       43.61234            0

SURFACE DATA DETAIL:

Surface OBJ     : STANDARD
Surface   1     : STANDARD
Surface   2     : STANDARD
 Aperture       : Circular Aperture
 Minimum Radius :            0
 Maximum Radius :          8.5
Surface   3     : STANDARD
Surface   4     : STANDARD
Surface   5     : STANDARD
Surface STO     : STANDARD
Surface   7     : STANDARD
Surface   8     : STANDARD
 Aperture       : Circular Aperture
 Minimum Radius :            0
 Maximum Radius :          7.5
Surface   9     : STANDARD
Surface IMA     : STANDARD

SOLVE AND VARIABLE DATA:

Curvature of   2   : Variable
Semi Diam   2      : Fixed
Curvature of   3   : Variable
Thickness of   3   : Variable
Semi Diam   3      : Fixed
Curvature of   4   : Variable
Semi Diam   4      : Fixed
Curvature of   5   : Variable
Semi Diam   5      : Fixed
Thickness of   6   : Variable
Curvature of   7   : Variable
Semi Diam   7      : Fixed
Curvature of   8   : Variable
Thickness of   8   : Solve, marginal ray height = 0.00000
Semi Diam   8      : Fixed

INDEX OF REFRACTION DATA:

Surf      Glass       0.450000    0.500000    0.550000    0.600000    0.650000
   0              1.00000000  1.00000000  1.00000000  1.00000000  1.00000000
   1              1.00000000  1.00000000  1.00000000  1.00000000  1.00000000
   2     LAFN21   1.80620521  1.79788762  1.79184804  1.78728036  1.78370773
   3              1.00000000  1.00000000  1.00000000  1.00000000  1.00000000
   4       SF53   1.75665336  1.74309602  1.73366378  1.72676633  1.72152789
   5              1.00000000  1.00000000  1.00000000  1.00000000  1.00000000
   6              1.00000000  1.00000000  1.00000000  1.00000000  1.00000000
   7     LAFN21   1.80620521  1.79788762  1.79184804  1.78728036  1.78370773
   8              1.00000000  1.00000000  1.00000000  1.00000000  1.00000000
   9              1.00000000  1.00000000  1.00000000  1.00000000  1.00000000
  10              1.00000000  1.00000000  1.00000000  1.00000000  1.00000000

ELEMENT VOLUME DATA:

Units are cubic cm.
Values are only accurate for plane and spherical surfaces.
Element surf   2 to   3 volume :       0.610995
Element surf   4 to   5 volume :       0.269441
Element surf   7 to   8 volume :       0.433018
```

Listing B.3.1.4 (continued)

by deleting the vignetted rays from a set of incident rays. This deletion has the subtle side effect of reducing the working weights on the fields with more vignetting and fewer transmitted rays. Fewer rays yield fewer optimization operands. Fewer operands make less of a contribution to the damped least-squares solution.

Merit Function Listing

File : C:LENS314B.ZMX
Title: COOKE TRIPLET, 52MM, F/3.5, 45.2DEG

Merit Function Value: 7.50829989E-003

Num	Type	Int1	Int2	Hx	Hy	Px	Py	Target	Weight	Value	% Cont
1	EFFL		3					5.20000E+001	1e+005	5.20001E+001	0.005
2	BLNK										
3	BLNK										
4	TTHI	3	3					0.00000E+000	0	4.01727E+000	0.000
5	TTHI	5	6					0.00000E+000	0	7.19832E+000	0.000
6	DIFF	5	4					0.00000E+000	0	3.18105E+000	0.000
7	OPGT	6						1.50000E+000	1e+005	1.50000E+000	0.000
8	BLNK										
9	BLNK										
10	DIST	0	3					0.00000E+000	1e+005	7.33768E-006	0.000
11	BLNK										
12	BLNK										
13	DMFS										
14	OPDC		1	0.0000	0.0000	0.2500	0.2500	0.00000E+000	0.8	8.28033E-003	0.000
15	OPDC		1	0.0000	0.0000	0.2500	0.7500	0.00000E+000	0.8	-1.93433E-001	0.177
16	OPDC		1	0.0000	0.0000	0.7500	0.2500	0.00000E+000	0.8	-1.93433E-001	0.177
17	OPDC		2	0.0000	0.0000	0.2500	0.2500	0.00000E+000	0.8	8.69492E-002	0.036
18	OPDC		2	0.0000	0.0000	0.2500	0.7500	0.00000E+000	0.8	4.49848E-001	0.957
19	OPDC		2	0.0000	0.0000	0.7500	0.2500	0.00000E+000	0.8	4.49848E-001	0.957
20	OPDC		3	0.0000	0.0000	0.2500	0.2500	0.00000E+000	0.8	3.10335E-002	0.005
21	OPDC		3	0.0000	0.0000	0.2500	0.7500	0.00000E+000	0.8	3.05747E-001	0.442
22	OPDC		3	0.0000	0.0000	0.7500	0.2500	0.00000E+000	0.8	3.05747E-001	0.442
23	OPDC		4	0.0000	0.0000	0.2500	0.2500	0.00000E+000	0.8	-5.79185E-002	0.016
24	OPDC		4	0.0000	0.0000	0.2500	0.7500	0.00000E+000	0.8	-6.32398E-002	0.019
25	OPDC		4	0.0000	0.0000	0.7500	0.2500	0.00000E+000	0.8	-6.32398E-002	0.019
26	OPDC		5	0.0000	0.0000	0.2500	0.2500	0.00000E+000	0.8	-1.48682E-001	0.105
27	OPDC		5	0.0000	0.0000	0.2500	0.7500	0.00000E+000	0.8	-4.74652E-001	1.066
28	OPDC		5	0.0000	0.0000	0.7500	0.2500	0.00000E+000	0.8	-4.74652E-001	1.066
29	OPDC		1	0.0000	0.3982	0.2500	-0.7500	0.00000E+000	0.3	-1.07468E+000	2.048
30	OPDC		1	0.0000	0.3982	0.2500	-0.2500	0.00000E+000	0.3	8.80501E-002	0.014
31	OPDC		1	0.0000	0.3982	0.2500	0.2500	0.00000E+000	0.3	2.50417E-001	0.111
32	OPDC		1	0.0000	0.3982	0.2500	0.7500	0.00000E+000	0.3	9.56563E-003	0.000
33	OPDC		1	0.0000	0.3982	0.7500	-0.2500	0.00000E+000	0.3	7.60901E-001	1.027
34	OPDC		1	0.0000	0.3982	0.7500	0.2500	0.00000E+000	0.3	1.18858E+000	2.506
35	OPDC		2	0.0000	0.3982	0.2500	-0.7500	0.00000E+000	0.3	-1.67402E-001	0.050
36	OPDC		2	0.0000	0.3982	0.2500	-0.2500	0.00000E+000	0.3	2.29260E-001	0.093
37	OPDC		2	0.0000	0.3982	0.2500	0.2500	0.00000E+000	0.3	2.18183E-001	0.084
38	OPDC		2	0.0000	0.3982	0.2500	0.7500	0.00000E+000	0.3	3.01055E-001	0.161
39	OPDC		2	0.0000	0.3982	0.7500	-0.2500	0.00000E+000	0.3	1.39278E+000	3.441
40	OPDC		2	0.0000	0.3982	0.7500	0.2500	0.00000E+000	0.3	1.60406E+000	4.564
41	OPDC		3	0.0000	0.3982	0.2500	-0.7500	0.00000E+000	0.3	-2.28682E-001	0.093
42	OPDC		3	0.0000	0.3982	0.2500	-0.2500	0.00000E+000	0.3	1.71230E-001	0.052
43	OPDC		3	0.0000	0.3982	0.2500	0.2500	0.00000E+000	0.3	1.31326E-001	0.031
44	OPDC		3	0.0000	0.3982	0.2500	0.7500	0.00000E+000	0.3	6.06463E-002	0.007
45	OPDC		3	0.0000	0.3982	0.7500	-0.2500	0.00000E+000	0.3	1.18771E+000	2.502
46	OPDC		3	0.0000	0.3982	0.7500	0.2500	0.00000E+000	0.3	1.33141E+000	3.144
47	OPDC		4	0.0000	0.3982	0.2500	-0.7500	0.00000E+000	0.3	-5.82113E-001	0.601
48	OPDC		4	0.0000	0.3982	0.2500	-0.2500	0.00000E+000	0.3	5.92456E-002	0.006
49	OPDC		4	0.0000	0.3982	0.2500	0.2500	0.00000E+000	0.3	4.09036E-002	0.003
50	OPDC		4	0.0000	0.3982	0.2500	0.7500	0.00000E+000	0.3	-3.06883E-001	0.167
51	OPDC		4	0.0000	0.3982	0.7500	-0.2500	0.00000E+000	0.3	7.46006E-001	0.987
52	OPDC		4	0.0000	0.3982	0.7500	0.2500	0.00000E+000	0.3	8.79151E-001	1.371
53	OPDC		5	0.0000	0.3982	0.2500	-0.7500	0.00000E+000	0.3	-1.00425E+000	1.789
54	OPDC		5	0.0000	0.3982	0.2500	-0.2500	0.00000E+000	0.3	-6.03986E-002	0.006
55	OPDC		5	0.0000	0.3982	0.2500	0.2500	0.00000E+000	0.3	-4.01545E-002	0.003
56	OPDC		5	0.0000	0.3982	0.2500	0.7500	0.00000E+000	0.3	-6.78202E-001	0.816
57	OPDC		5	0.0000	0.3982	0.7500	-0.2500	0.00000E+000	0.3	2.62630E-001	0.122
58	OPDC		5	0.0000	0.3982	0.7500	0.2500	0.00000E+000	0.3	4.08174E-001	0.296
59	OPDC		1	0.0000	0.6991	0.2500	-0.2500	0.00000E+000	0.2	2.91949E-001	0.101
60	OPDC		1	0.0000	0.6991	0.2500	0.2500	0.00000E+000	0.2	3.83947E-001	0.174
61	OPDC		1	0.0000	0.6991	0.2500	0.7500	0.00000E+000	0.2	-1.75633E+000	3.648
62	OPDC		1	0.0000	0.6991	0.7500	-0.2500	0.00000E+000	0.2	1.60934E+000	3.063
63	OPDC		1	0.0000	0.6991	0.7500	0.2500	0.00000E+000	0.2	1.95819E+000	4.534
64	OPDC		2	0.0000	0.6991	0.2500	-0.2500	0.00000E+000	0.2	4.02041E-001	0.191
65	OPDC		2	0.0000	0.6991	0.2500	0.2500	0.00000E+000	0.2	2.71910E-001	0.087
66	OPDC		2	0.0000	0.6991	0.2500	0.7500	0.00000E+000	0.2	-1.67794E+000	3.329
67	OPDC		2	0.0000	0.6991	0.7500	-0.2500	0.00000E+000	0.2	2.15371E+000	5.485
68	OPDC		2	0.0000	0.6991	0.7500	0.2500	0.00000E+000	0.2	2.24437E+000	5.956
69	OPDC		3	0.0000	0.6991	0.2500	-0.2500	0.00000E+000	0.2	2.97159E-001	0.104
70	OPDC		3	0.0000	0.6991	0.2500	0.2500	0.00000E+000	0.2	1.67794E-001	0.033
71	OPDC		3	0.0000	0.6991	0.2500	0.7500	0.00000E+000	0.2	-1.89446E+000	4.244
72	OPDC		3	0.0000	0.6991	0.7500	-0.2500	0.00000E+000	0.2	1.86086E+000	4.095
73	OPDC		3	0.0000	0.6991	0.7500	0.2500	0.00000E+000	0.2	1.91078E+000	4.317
74	OPDC		4	0.0000	0.6991	0.2500	-0.2500	0.00000E+000	0.2	1.40219E-001	0.023
75	OPDC		4	0.0000	0.6991	0.2500	0.2500	0.00000E+000	0.2	8.22733E-002	0.008
76	OPDC		4	0.0000	0.6991	0.2500	0.7500	0.00000E+000	0.2	-2.15451E+000	5.489
77	OPDC		4	0.0000	0.6991	0.7500	-0.2500	0.00000E+000	0.2	1.34077E+000	2.126
78	OPDC		4	0.0000	0.6991	0.7500	0.2500	0.00000E+000	0.2	1.42478E+000	2.400
79	OPDC		5	0.0000	0.6991	0.2500	-0.2500	0.00000E+000	0.2	-1.87010E-002	0.000
80	OPDC		5	0.0000	0.6991	0.2500	0.2500	0.00000E+000	0.2	1.39299E-002	0.000
81	OPDC		5	0.0000	0.6991	0.2500	0.7500	0.00000E+000	0.2	-2.39172E+000	6.764
82	OPDC		5	0.0000	0.6991	0.7500	-0.2500	0.00000E+000	0.2	7.89234E-001	0.737
83	OPDC		5	0.0000	0.6991	0.7500	0.2500	0.00000E+000	0.2	9.32214E-001	1.028
84	OPDC		1	0.0000	1.0000	0.2500	-0.2500	0.00000E+000	0.1	1.73150E+000	1.773
85	OPDC		1	0.0000	1.0000	0.2500	0.2500	0.00000E+000	0.1	3.86223E-001	0.088
86	OPDC		1	0.0000	1.0000	0.7500	0.2500	0.00000E+000	0.1	-2.10541E+000	2.621
87	OPDC		2	0.0000	1.0000	0.2500	-0.2500	0.00000E+000	0.1	1.24723E+000	0.920
88	OPDC		2	0.0000	1.0000	0.2500	0.2500	0.00000E+000	0.1	3.24755E-001	0.062
89	OPDC		2	0.0000	1.0000	0.7500	0.2500	0.00000E+000	0.1	-1.31885E+000	1.028
90	OPDC		3	0.0000	1.0000	0.2500	-0.2500	0.00000E+000	0.1	7.64997E-001	0.346
91	OPDC		3	0.0000	1.0000	0.2500	0.2500	0.00000E+000	0.1	2.79604E-001	0.046
92	OPDC		3	0.0000	1.0000	0.7500	0.2500	0.00000E+000	0.1	-1.23002E+000	0.895
93	OPDC		4	0.0000	1.0000	0.2500	-0.2500	0.00000E+000	0.1	3.57826E-001	0.076
94	OPDC		4	0.0000	1.0000	0.2500	0.2500	0.00000E+000	0.1	2.45048E-001	0.036
95	OPDC		4	0.0000	1.0000	0.7500	0.2500	0.00000E+000	0.1	-1.36724E+000	1.105
96	OPDC		5	0.0000	1.0000	0.2500	-0.2500	0.00000E+000	0.1	2.66086E-002	0.000
97	OPDC		5	0.0000	1.0000	0.2500	0.2500	0.00000E+000	0.1	2.17879E-001	0.028
98	OPDC		5	0.0000	1.0000	0.7500	0.2500	0.00000E+000	0.1	-1.57081E+000	1.459

Listing B.3.2.1

This complication is another reason why the lens designer may wish to experiment with field weights.

Figure B.3.2.1 is the layout of the final OPD optimized Cooke Triplet. Note that the general configuration is very similar to the spot size optimized lens in Figure B.3.1.1, but the front airspace is relatively smaller and the surface curves are somewhat different.

Figure B.3.2.2 is the vignetting plot. Note that the fraction of unvignetted rays at the edge of the field is 0.47 or 47% (1.09 stops down from the field center). This throughput value is close enough to the 50% target.

However, note that the vignetting diagram in Figure B.3.2.2 does not include the effect of cosine-fourth vignetting. Cosine-fourth vignetting darkens the edge of the field by an additional amount beyond any mechanical vignetting. For 22.6º off-axis, cosine-fourth is 0.73 or 73% (0.46 stops down from the field center). This value assumes negligible pupil growth from pupil aberrations, a reasonable assumption for a Cooke Triplet. Thus, total estimated light falloff from both types of vignetting gives relative illumination (irradiance) at the edge of the field of 0.34 or 34% 1.55 stops down from the field center). Again, this amount of light falloff will scarcely be noticed in practice.

Figure B.3.2.3 is the transverse ray fan plot; compare it to Figure B.3.1.4. Figure B.3.2.4 gives the field curvature and percent distortion plots; compare these with the plots in Figure B.3.1.5. Figure B.3.2.5 is the polychromatic spot diagram; compare this with Figure B.3.1.6. Clearly, Figures B.3.2.3 and B.3.2.5 show that the OPD optimized lens is worse when evaluated by transverse ray errors.

Figure B.3.2.6 is the OPD ray fan plot; compare it to Figure B.3.1.8. Now the OPD optimized lens is better. Note that there is still astigmatism, as revealed by the different curvatures at the origins of the tangential and sagittal off-axis plots. Note too that the astigmatism changes sign between the 70% field and the 100% field; this agrees with the field curvature plot where the curves cross near the 90% field.

Figure B.3.2.7 is the diffraction MTF plot; compare this with Figure B.3.1.9. Again the OPD optimized lens is better. Furthermore, the lens as optimized with OPD now gives a level of MTF performance that is acceptable for a normal, moderate speed 35 mm camera lens.

Camera lenses are often used stopped down. Figure B.3.2.8 is the MTF plot for the OPD optimized *f*/3.5 Cooke Triplet when stopped down to *f*/8. At this commonly used opening, image quality is quite good. However, the effects of the field-zonal astigmatism are still noticeable. Refer again to the field curvature plot in Figure B.3.2.4. At 70% field, the sagittal image surface is quite far from the actual image surface, and thus the sagittal MTF is degraded. At 100% field, past the tangential-sagittal curve crossing, the tangential image surface is now quite far from the actual image surface, and thus now the tangential MTF suffers.

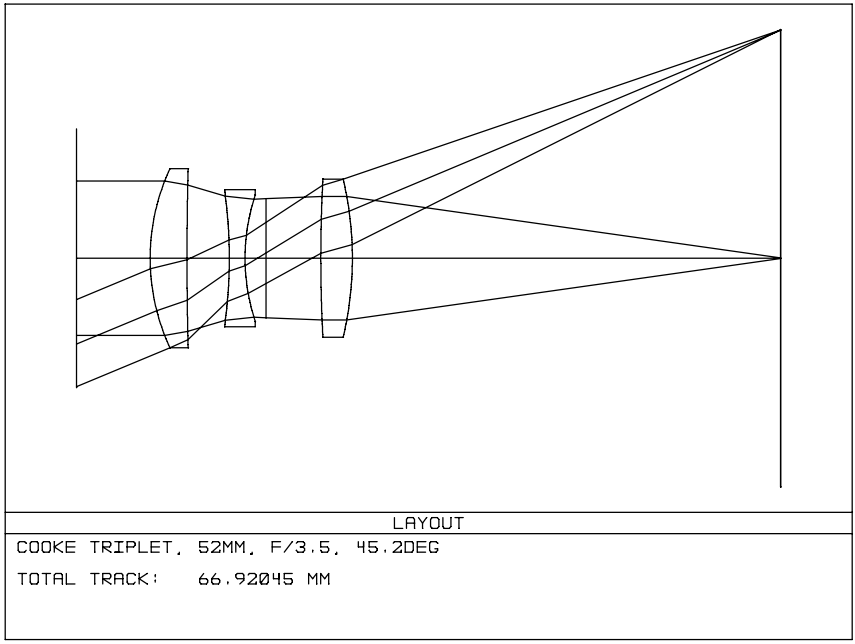

Figure B.3.2.1

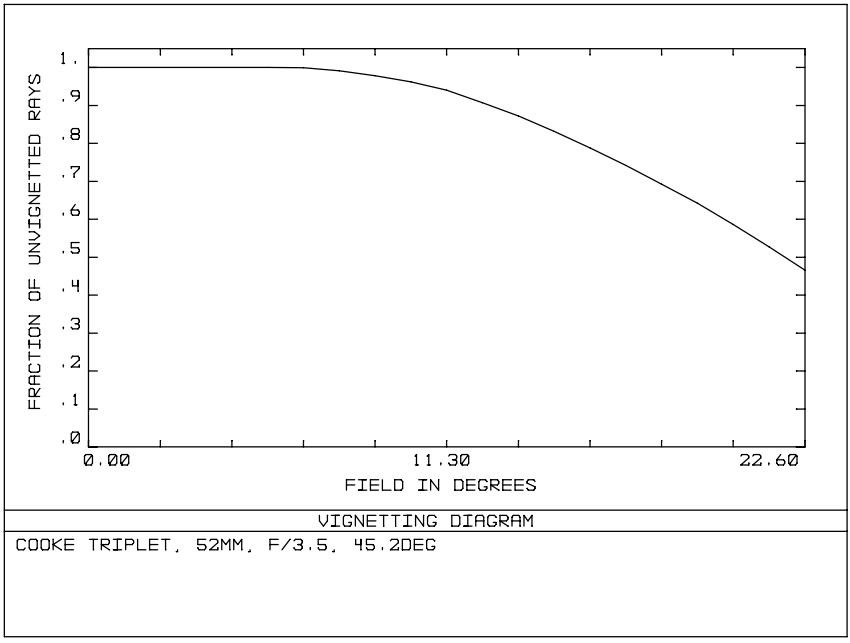

Figure B.3.2.2

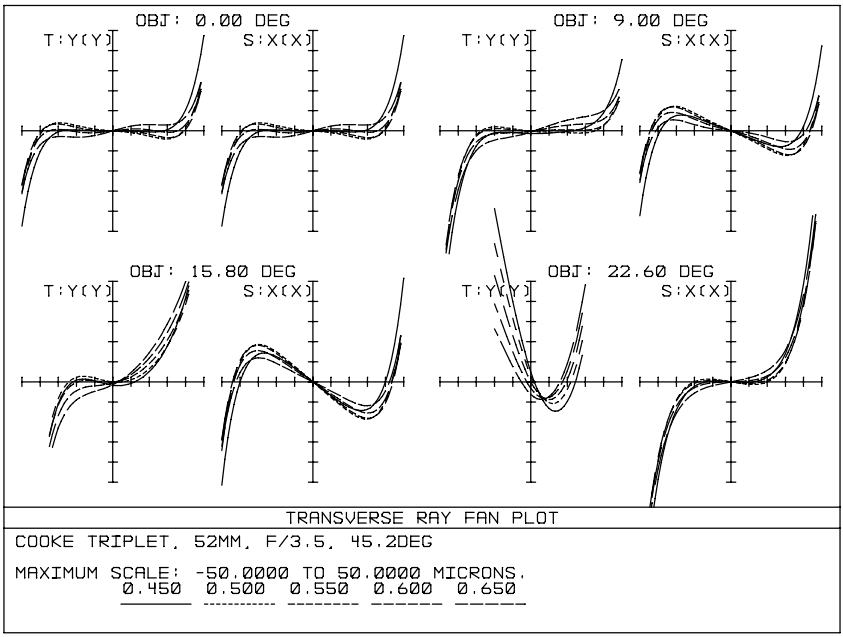

Figure B.3.2.3

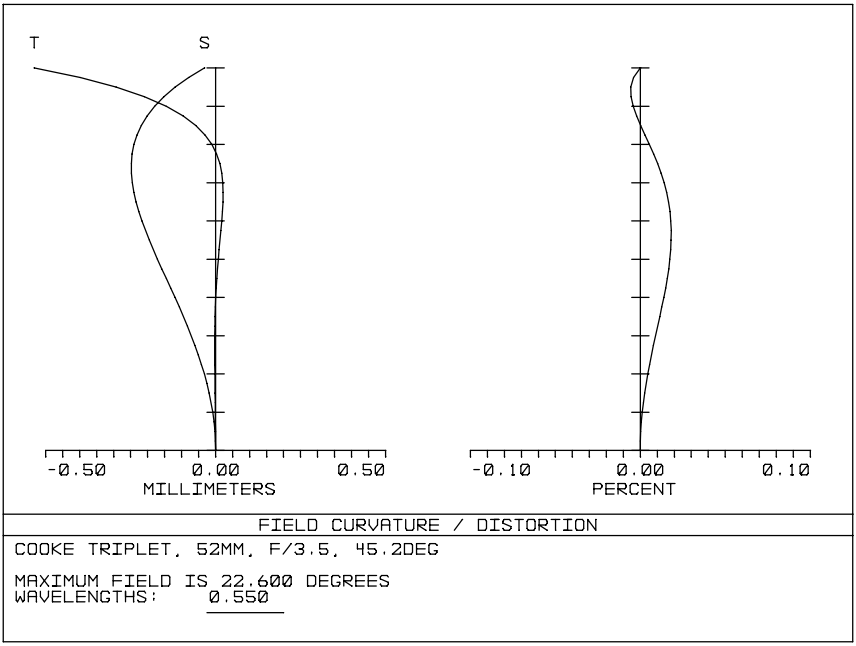

Figure B.3.2.4

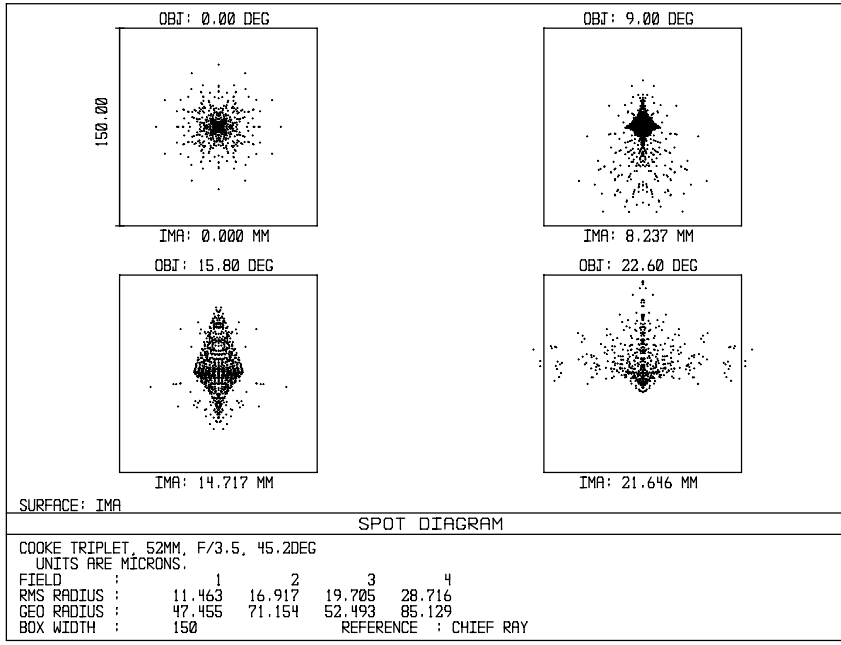

Figure B.3.2.5

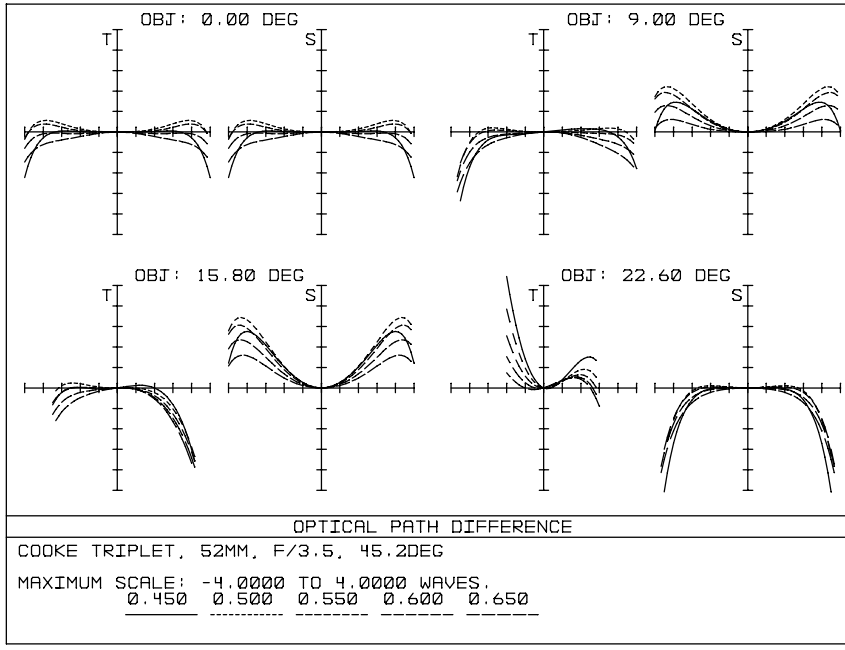

Figure B.3.2.6

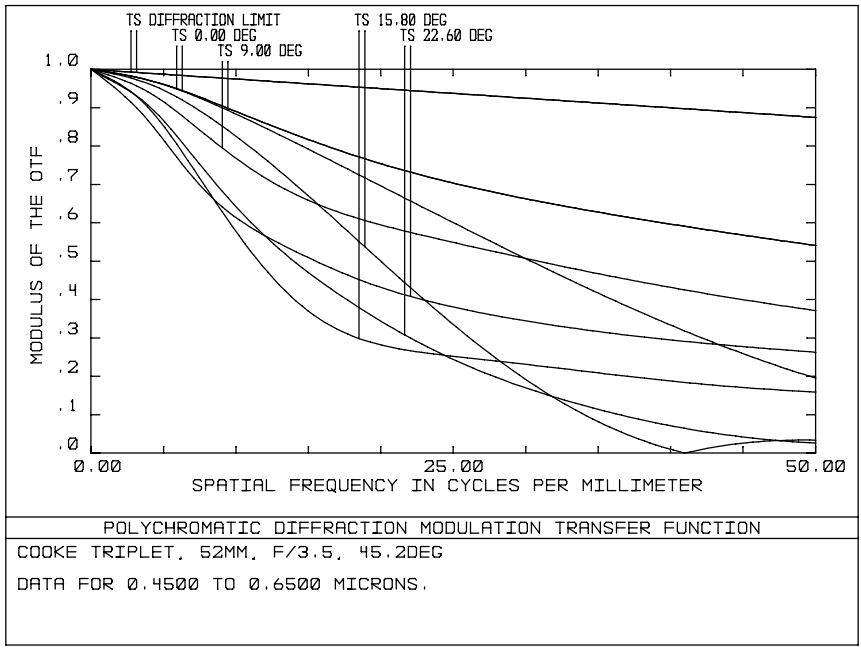

Figure B.3.2.7 Lens wide open.

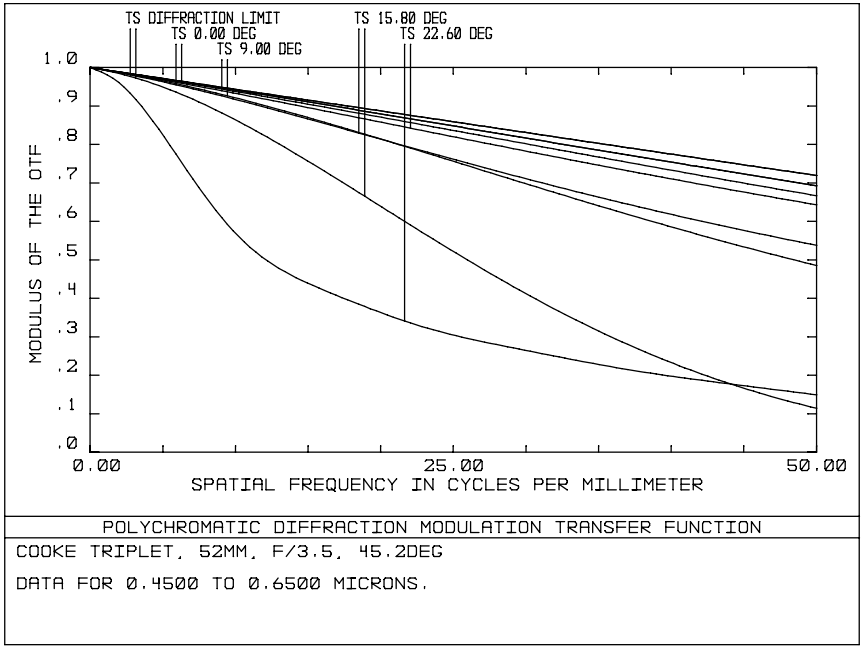

Figure B.3.2.8 Lens stopped down to *f*/8.

Finally, Listing B.3.2.2 gives the optical prescription for the OPD optimized Cooke Triplet.

B.3.3 The Tessar Lens

If you require a bit more optical performance than the Cooke Triplet can deliver, then the four element Tessar configuration, illustrated in Figure B.3.3.1, may be the answer. Clearly, the Tessar, whose name derives from the Greek word meaning four, closely resembles the Cooke Triplet. The big difference is that the rear singlet in the Cooke Triplet has been replaced by a cemented doublet. The additional element gives the lens designer one more surface curvature to vary during optimization to control aberrations. With the Tessar, there are nine effective independent variables: seven curvatures and two airspaces. Once again, the glass thicknesses are only weak, ineffective variables and are fixed at practical values. Of course, glass selection is still very important.

The lens shown here is the classic Tessar with the outside element of the doublet having positive power. There is a Tessar derivative where the positive and negative elements of the doublet are reversed in order. There is still another derivative where the whole lens is reversed. The performance of all three versions is about the same. By far, the majority of Tessars are the classic variety.

In the present Tessar example, the basic lens specifications are the same as in the Cooke Triplet example. This includes the same amount of vignetting. The idea is to create two designs that can be directly compared. Once again, MTF is the image quality criterion.

The Tessar is not strictly symmetrical, but nevertheless the design still contains much symmetry. This symmetry can help in deriving a starting configuration. In addition, a look at published Tessar layouts will suggest some useful initial constraints that can shepherd the lens in the right direction. Make the inside surface of the front element flat. Make the two curvatures of the singlet negative element equal with opposite signs. Make the inside air-to-glass surface of the doublet flat. Make the two curvatures of the positive element of the doublet equal with opposite signs. And make the front airspace equal to the space between the stop and the first surface of the cemented doublet. Use pickups for the coupled parameters. For glasses, make a guess based on published accounts (see below for more on glass). It is no accident that to a large extent this starting configuration looks very much like a Cooke Triplet.

With these constraints, you optimize as you did for the Cooke Triplet. Focal length is corrected to 52 mm, paraxial longitudinal color is corrected to zero, and polychromatic spot sizes are reduced. Ignore distortion for now. If the airspaces become too large or too small, change the glass for the negative singlet and reoptimize. The resulting lens configuration will be good enough for use at the start of the intermediate optimizations (with the initial constraints removed, of course).

Listing B.3.2.2

```
System/Prescription Data

File : C:LENS314B.ZMX
Title: COOKE TRIPLET, 52MM, F/3.5, 45.2DEG

GENERAL LENS DATA:

Surfaces         :          10
Stop             :           6
System Aperture :Entrance Pupil Diameter
Ray aiming       : On
 X Pupil shift   : 0
 Y Pupil shift   : 0
 Z Pupil shift   : 0
Apodization      :Uniform, factor =     0.000000
Eff. Focal Len.  :      52.0001 (in air)
Eff. Focal Len.  :      52.0001 (in image space)
Total Track      :      66.9205
Image Space F/# :      3.49933
Para. Wrkng F/# :      3.49933
Working F/#      :      3.56044
Obj. Space N.A. :   7.43e-010
Stop Radius      :      5.65521
Parax. Ima. Hgt.:      21.6455
Parax. Mag.      :            0
Entr. Pup. Dia.  :        14.86
Entr. Pup. Pos.  :      19.7086
Exit Pupil Dia.  :      14.0556
Exit Pupil Pos.  :     -49.1852
Field Type       : Angle in degrees
Maximum Field    :         22.6
Primary Wave     :     0.550000
Lens Units       : Millimeters
Angular Mag.     :      1.05723

Fields           : 4
Field Type:  Angle in degrees
#          X-Value          Y-Value          Weight
1         0.000000         0.000000         4.000000
2         0.000000         9.000000         3.000000
3         0.000000        15.800000         2.000000
4         0.000000        22.600000         1.000000

Vignetting Factors
#          VDX              VDY              VCX              VCY
1         0.000000         0.000000         0.000000         0.000000
2         0.000000         0.000000         0.000000         0.000000
3         0.000000         0.000000         0.000000         0.000000
4         0.000000         0.000000         0.000000         0.000000

Wavelengths     : 5
Units:  Microns
#          Value          Weight
1         0.450000         1.000000
2         0.500000         1.000000
3         0.550000         1.000000
4         0.600000         1.000000
5         0.650000         1.000000

SURFACE DATA SUMMARY:

Surf      Type         Radius       Thickness          Glass      Diameter         Conic
 OBJ  STANDARD       Infinity        Infinity                          0              0
   1  STANDARD       Infinity               7                   33.76985              0
   2  STANDARD       20.21304             3.5         LAFN21          17              0
   3  STANDARD       357.8886         4.01727                         17              0
   4  STANDARD      -46.76389             1.5           SF53          13              0
   5  STANDARD       18.91477               2                         12              0
 STO  STANDARD       Infinity         5.198322                    11.31043            0
   7  STANDARD        142.092               3         LAFN21          15              0
   8  STANDARD      -32.48564         40.70486                        15              0
   9  STANDARD       Infinity                0                    43.7664             0
 IMA  STANDARD       Infinity                0                    43.7664             0

SURFACE DATA DETAIL:

Surface OBJ     : STANDARD
Surface   1     : STANDARD
Surface   2     : STANDARD
 Aperture       : Circular Aperture
 Minimum Radius :            0
 Maximum Radius :          8.5
Surface   3     : STANDARD
Surface   4     : STANDARD
Surface   5     : STANDARD
Surface STO     : STANDARD
Surface   7     : STANDARD
Surface   8     : STANDARD
 Aperture       : Circular Aperture
 Minimum Radius :            0
 Maximum Radius :          7.5
Surface   9     : STANDARD
Surface IMA     : STANDARD

SOLVE AND VARIABLE DATA:

Curvature of   2   : Variable
Semi Diam   2      : Fixed
Curvature of   3   : Variable
Thickness of   3   : Variable
Semi Diam   3      : Fixed
Curvature of   4   : Variable
Semi Diam   4      : Fixed
Curvature of   5   : Variable
Semi Diam   5      : Fixed
Thickness of   6   : Variable
Curvature of   7   : Variable
Semi Diam   7      : Fixed
Curvature of   8   : Variable
Thickness of   8   : Solve, marginal ray height = 0.00000
Semi Diam   8      : Fixed

INDEX OF REFRACTION DATA:

Surf     Glass      0.450000    0.500000    0.550000    0.600000    0.650000
   0              1.00000000  1.00000000  1.00000000  1.00000000  1.00000000
   1              1.00000000  1.00000000  1.00000000  1.00000000  1.00000000
   2     LAFN21   1.80620521  1.79788762  1.79184804  1.78728036  1.78370773
   3              1.00000000  1.00000000  1.00000000  1.00000000  1.00000000
   4       SF53   1.75655336  1.74309602  1.73366378  1.72676633  1.72152789
   5              1.00000000  1.00000000  1.00000000  1.00000000  1.00000000
   6              1.00000000  1.00000000  1.00000000  1.00000000  1.00000000
   7     LAFN21   1.80620521  1.79788762  1.79184804  1.78728036  1.78370773
   8              1.00000000  1.00000000  1.00000000  1.00000000  1.00000000
   9              1.00000000  1.00000000  1.00000000  1.00000000  1.00000000
  10              1.00000000  1.00000000  1.00000000  1.00000000  1.00000000

ELEMENT VOLUME DATA:

Units are cubic cm.
Values are only accurate for plane and spherical surfaces.
Element surf   2 to   3 volume :       0.596651
Element surf   4 to   5 volume :       0.273760
Element surf   7 to   8 volume :       0.435456
```

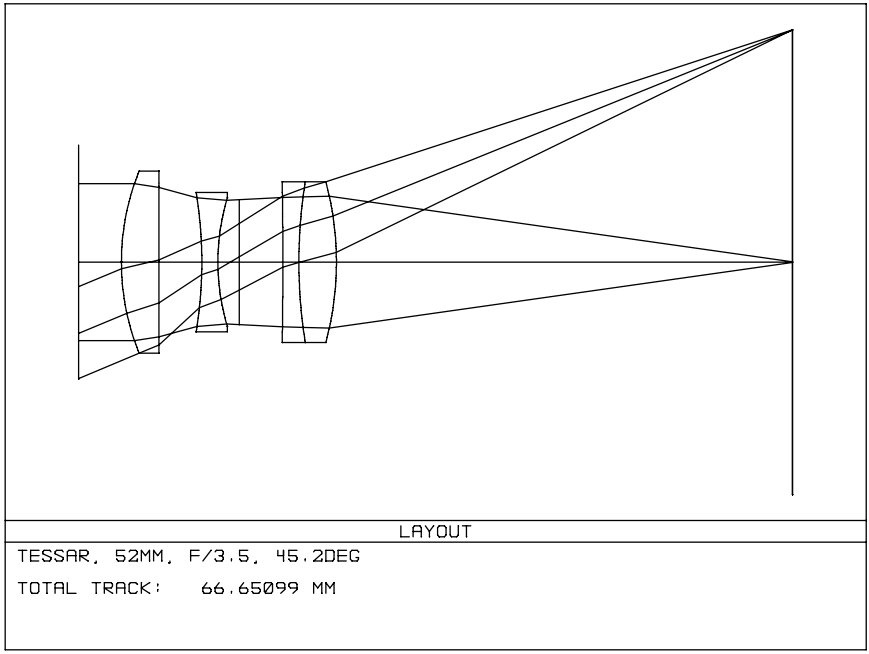

Figure B.3.3.1

The biggest issue throughout the design of a Tessar is glass selection. The one thing that is clear is that for best results, the positive elements should be made of high-index crown glass. The reasons are the same as those outlined for the Cooke Triplet: crown glass for achromatization, and high index to reduce the naturally negative Petzval sum and to reduce higher-order aberrations. Older Tessar designs use the barium crowns (the SK glasses in the Schott catalog). Newer Tessars use the even higher-index lanthanum crowns.

Thus, the problem becomes selecting the glasses for the two negative elements. Most published accounts suggest that relative to the crowns, both negative elements be flints and be selected from the glasses along the old glass line. The negative singlet usually has a somewhat lower index and is very flinty relative to the crowns. The cemented negative element usually has a much lower index and is only moderately more flinty relative to the crowns.

But this approach is not universal. The famous 50 mm *f*/3.5 Elmar lens for the original Leica camera is a Tessar derivative with the stop in the front airspace rather than the rear airspace. In order from front to rear, the glasses for the Elmar are: SK7, F5, BK7, and SK15.[3] Relative to SK15 (n_d of 1.623, V_d of 58.1), BK7 (n_d of 1.517, V_d of 64.2) is a crown, not a flint. In fact, it is possible to design ex-

[3] Dierick Kossel, "Glass Compositions," *Leica Fotografie*, English edition, Feb. 1978, pp. 20-25.

cellent Tessars with equal dispersions for the two elements of the cemented doublet.

For the present Tessar example, the glass type adopted for both of the crowns is the same as for the crowns in the Cooke Triplet, Schott LaFN21. However, when the computer is asked to find the matching glasses for the negative elements, the results are inconclusive. To understand this behavior, a manual approach is used. Four separate Tessars were optimized with the glass for the cemented negative element fixed successively at LLF2, F5, SF2, and SF15. For each case, a matching flint for the negative singlet was found by a search along the old glass line and by repeatedly optimizing with the intermediate merit function. The remarkable result is that all four solutions give almost identical optical performance. No wonder the automatic glass selection is inconclusive.

Thus, Schott F5 (n_d of 1.603, V_d of 38.0) is arbitrarily adopted for the negative cemented element. The reason is historical; relative to LaFN21 (n_d of 1.788, V_d of 47.5), F5 has the classical position on the glass map, down and to the right. The matching flint is found to be Schott SF15 (n_d of 1.699, V_d of 30.1). Thus, the glass set for the Tessar becomes: LaFN21, SF15, F5, LaFN21. These are all preferred glasses.

The intermediate and final optimizations for a Tessar are very similar to those for a Cooke Triplet. During the final optimizations, both a spot size optimization and an OPD optimization are done. MTFs are plotted and the results compared. As with the Cooke Triplet, the OPD optimized Tessar is found to give better MTF performance.

Figure B.3.3.1 shows the layout of the final OPD optimized Tessar. Note that the inside surface of the front element and the air-to glass surface of the cemented negative element are both nearly flat. If this Tessar were to be actually fabricated, one or both of these surfaces would probably be made exactly flat and the lens reoptimized with little loss of performance. Surfaces with very long radii are hard to make and are often not worth the effort.

Figure B.3.3.2 is the vignetting plot of geometrical throughput versus field angle for the Tessar. Note that the fraction of unvignetted rays at the edge of the field is 0.48 or 48% (1.06 stops down from the field center). This value is nearly identical to the corresponding value for the Cooke Triplet as shown on Figure B.3.2.2.

Figure B.3.3.3 shows the transverse ray fan plots for the Tessar. Compare these to the plots in Figure B.3.2.3 for the Cooke Triplet. Clearly, the two sets of curves are very similar. The most noticeable difference is that the off-axis tangential curves for the Tessar show somewhat smaller ray errors. Like the Triplet, the Tessar suffers from off-axis oblique spherical aberration and field-zonal astigmatism.

Figure B.3.3.4 shows the field curvature and percent distortion plots. Compare these to the plots in Figure B.3.2.4. On the left, note that the Tessar has no-

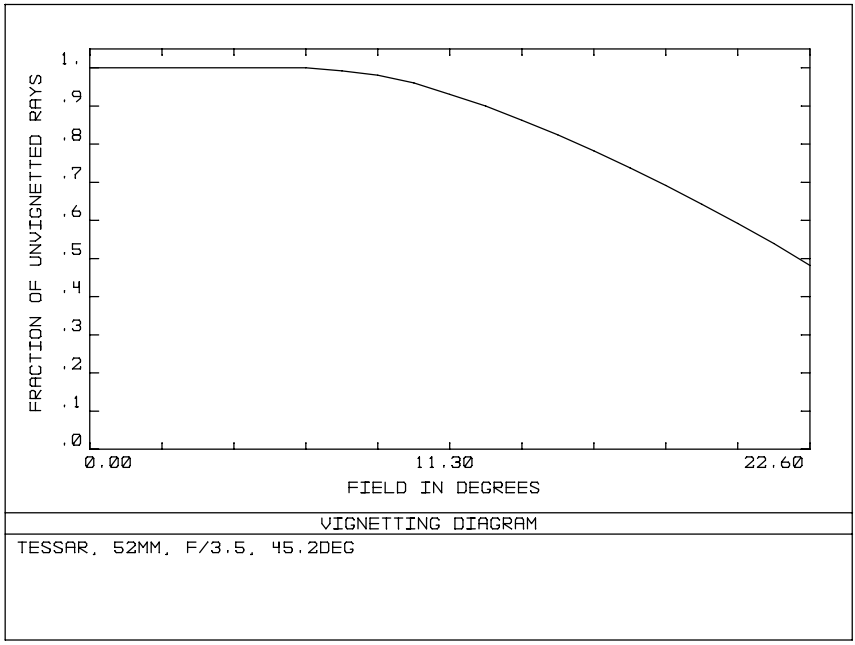

Figure B.3.3.2

ticeably less field-zonal astigmatism than the Cooke Triplet. Consequently, the Tessar needs less emphasis on the intermediate field positions during optimization. The field weights of 4 3 2 1 for the Triplet were changed to 5 4 3 2 for the Tessar. On the right, note that like the Cooke Triplet, distortion in the Tessar has been corrected to zero at the edge of the field by balancing third-order distortion with higher-orders. Note too that at intermediate fields there is a small amount of residual third-order distortion of little or no practical consequence.

Figure B.3.3.5 gives the polychromatic spot diagrams. Compare these to Figure B.3.2.5. As with the ray fan plots, the spots indicate that the Tessar and Triplet have very similar geometrical performance. Qualitatively, the spot shapes are nearly the same; quantitatively, the spot sizes are somewhat less for the Tessar. Thus, the Tessar is definitely the better lens, although only moderately so.

Figure B.3.3.6 gives the OPD ray fan plots. Compare these to Figure B.3.2.6. Again the Tessar is somewhat better.

Figure B.3.3.7 gives the MTF curves for the Tessar wide open at *f*/3.5. Compare these with the MTF curves in Figure B.3.2.7 for the Cooke Triplet, also wide open at *f*/3.5. Clearly, the Tessar has higher performance, but again the advantage is not great. However, this modest advantage may be the difference between success and failure in the marketplace. Accordingly, many lens makers have chosen to expend the extra effort to add a fourth element to make a Tessar rather than a Cooke Triplet.

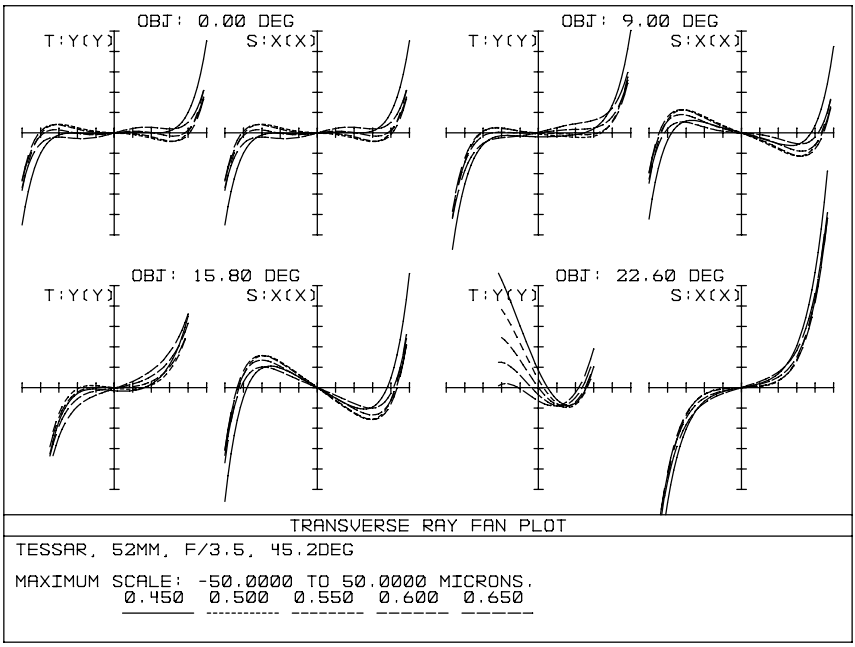

Figure B.3.3.3

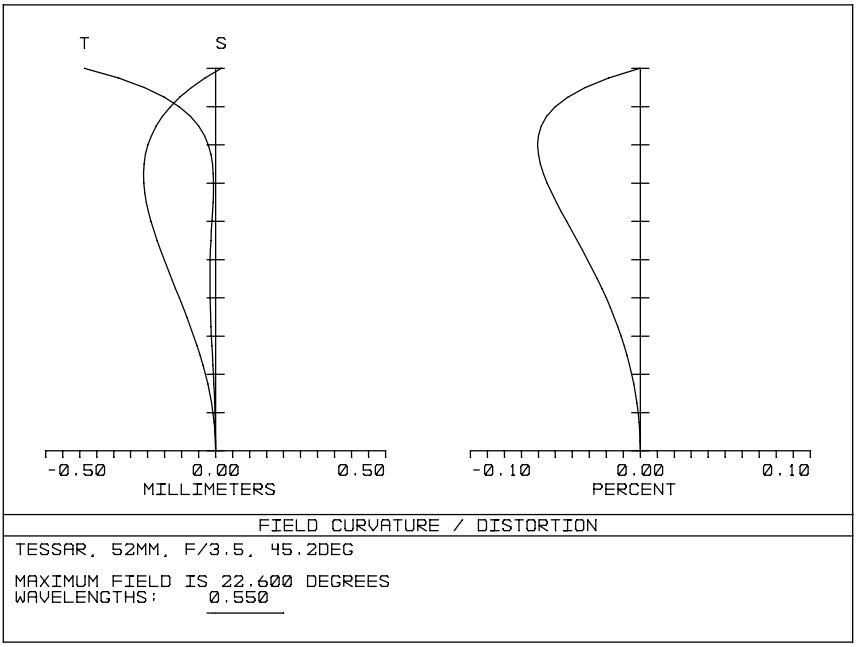

Figure B.3.3.4

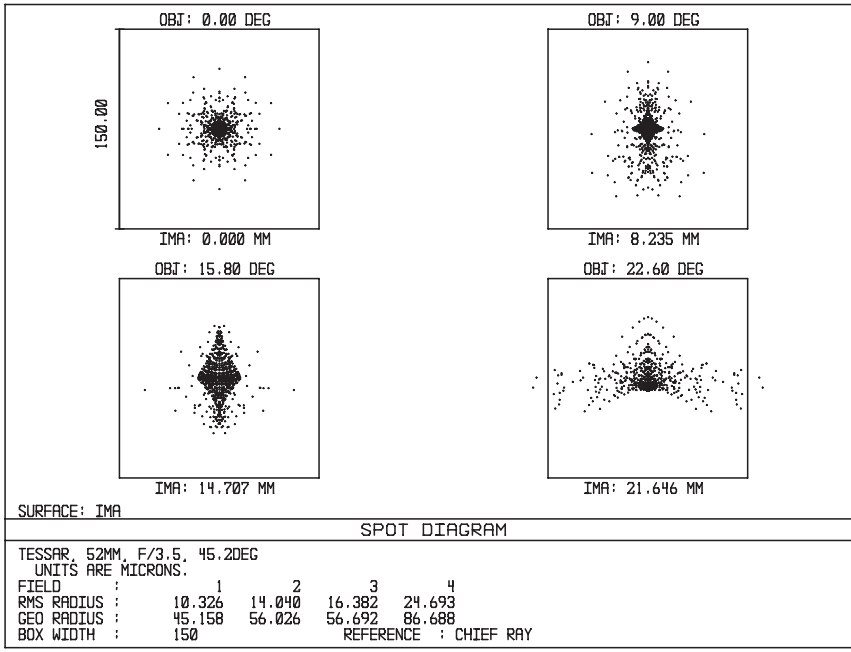

Figure B.3.3.5

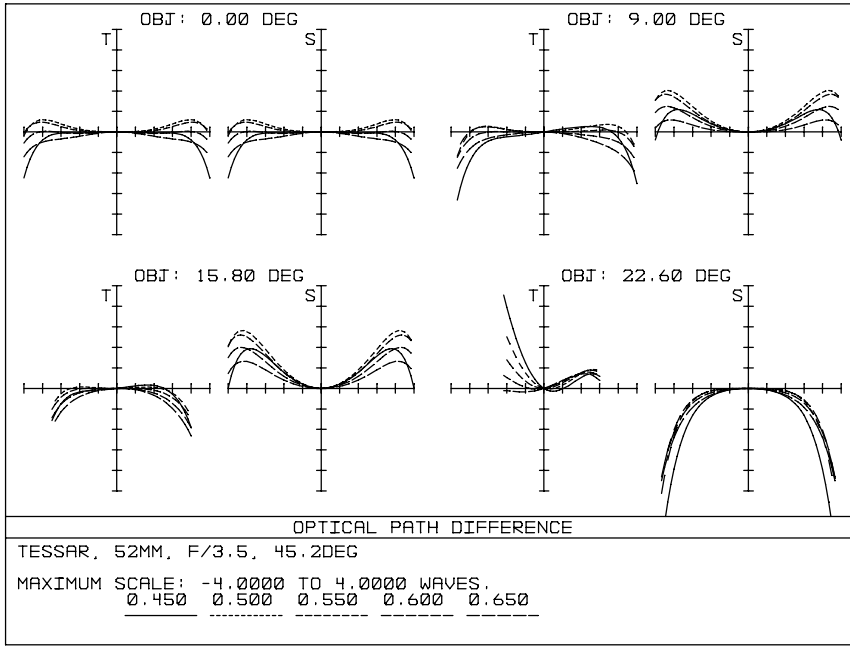

Figure B.3.3.6

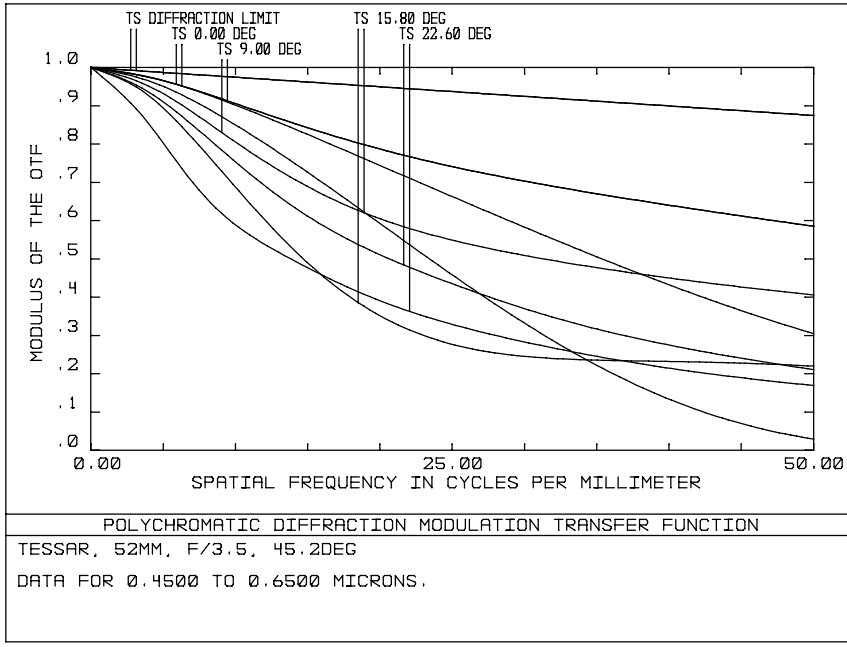

Figure B.3.3.7 Lens wide open.

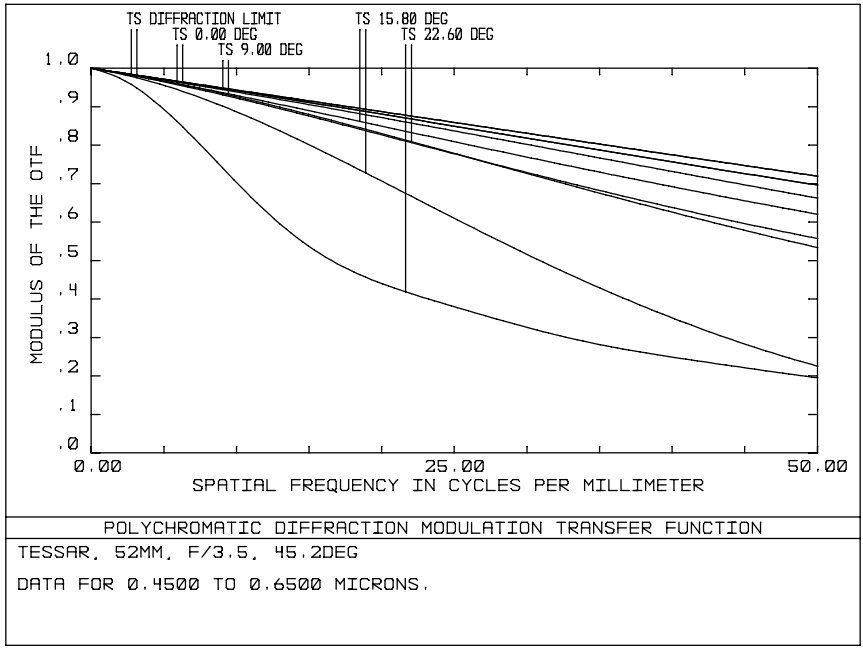

Figure B.3.3.8 Lens stopped down to *f*/8.

Figure B.3.3.8 gives the MTF curves for the Tessar when stopped down to *f*/8. Compare these with the MTF curves in Figure B.3.2.8 for the Cooke Triplet, also stopped down to *f*/8. In addition, compare the MTF performance of both lenses at *f*/8 versus *f*/3.5. Clearly, both the Tessar and Triplet have much better MTF performance at *f*/8 than at *f*/3.5. But this should be no surprise to any photographer who knows that his lens gets sharper when stopped down. When both lenses are at *f*/8, the Tessar is once again somewhat better than the Cooke Triplet.

Finally, Listing B.3.3 gives the optical prescription for the OPD optimized Tessar. This Tessar lens is toleranced in Chapter B.7.

The Cooke Triplet and Tessar lens configurations are two of the most popular in the world. But their speeds are limited. For a 35 mm camera, many photographers now insist on buying a faster standard lens. Over the years, several basic approaches to a fast lens have been tried. But only one is widely used today. This configuration is known among lens designers as the Double-Gauss. In the next chapter, the Double-Gauss lens will be examined, and its performance will be compared to that of the Cooke Triplet and Tessar.

```
System/Prescription Data

File : C:LENS324B.ZMX
Title: TESSAR, 52MM, F/3.5, 45.2DEG

GENERAL LENS DATA:

Surfaces         :          11
Stop             :           6
System Aperture :Entrance Pupil Diameter
Ray aiming       : On
 X Pupil shift   : 0
 Y Pupil shift   : 0
 Z Pupil shift   : 0
Apodization      :Uniform, factor =     0.000000
Eff. Focal Len. :      52.001 (in air)
Eff. Focal Len. :      52.001 (in image space)
Total Track      :      66.651
Image Space F/# :     3.49939
Para. Wrkng F/# :     3.49939
Working F/#      :     3.56248
Obj. Space N.A. :   7.43e-010
Stop Radius      :     5.82916
Parax. Ima. Hgt.:     21.6459
Parax. Mag.      :           0
Entr. Pup. Dia. :       14.86
Entr. Pup. Pos. :     16.2583
Exit Pupil Dia. :     14.6565
Exit Pupil Pos. :    -51.2887
Field Type       : Angle in degrees
Maximum Field    :        22.6
Primary Wave     :    0.550000
Lens Units       : Millimeters
Angular Mag.     :     1.01389


Fields           : 4
Field Type:  Angle in degrees
#          X-Value          Y-Value          Weight
1        0.000000         0.000000         5.000000
2        0.000000         9.000000         4.000000
3        0.000000        15.800000         3.000000
4        0.000000        22.600000         2.000000
```

Listing B.3.3

```
Vignetting Factors
#          VDX             VDY             VCX             VCY
1       0.000000        0.000000        0.000000        0.000000
2       0.000000        0.000000        0.000000        0.000000
3       0.000000        0.000000        0.000000        0.000000
4       0.000000        0.000000        0.000000        0.000000

Wavelengths     : 5
Units:  Microns
#            Value          Weight
1         0.450000        1.000000
2         0.500000        1.000000
3         0.550000        1.000000
4         0.600000        1.000000
5         0.650000        1.000000

SURFACE DATA SUMMARY:

Surf      Type        Radius       Thickness         Glass       Diameter         Conic
 OBJ   STANDARD      Infinity       Infinity                          0              0
   1   STANDARD      Infinity              4                    30.51105              0
   2   STANDARD       22.5851            3.5         LAFN21          17              0
   3   STANDARD      3174.661       4.005808                         17              0
   4   STANDARD     -39.77737            1.5          SF15          13              0
   5   STANDARD      20.74764              2                         12              0
 STO   STANDARD      Infinity        4.06086                    11.65832              0
   7   STANDARD     -502.9552            1.5           F5          15              0
   8   STANDARD      47.47455            3.5         LAFN21          15              0
   9   STANDARD     -28.85977       42.58433                         15              0
  10   STANDARD      Infinity              0                    43.63454              0
 IMA   STANDARD      Infinity              0                    43.63454              0

SURFACE DATA DETAIL:

Surface OBJ     : STANDARD
Surface   1     : STANDARD
Surface   2     : STANDARD
 Aperture       : Circular Aperture
 Minimum Radius :            0
 Maximum Radius :          8.5
Surface   3     : STANDARD
Surface   4     : STANDARD
Surface   5     : STANDARD
Surface STO     : STANDARD
Surface   7     : STANDARD
Surface   8     : STANDARD
Surface   9     : STANDARD
 Aperture       : Circular Aperture
 Minimum Radius :            0
 Maximum Radius :          7.5
Surface  10     : STANDARD
Surface IMA     : STANDARD

SOLVE AND VARIABLE DATA:

Curvature of   2   : Variable
Semi Diam   2      : Fixed
Curvature of   3   : Variable
Thickness of   3   : Variable
Semi Diam   3      : Fixed
Curvature of   4   : Variable
Semi Diam   4      : Fixed
Curvature of   5   : Variable
Semi Diam   5      : Fixed
Thickness of   6   : Variable
Curvature of   7   : Variable
Semi Diam   7      : Fixed
Curvature of   8   : Variable
Semi Diam   8      : Fixed
Curvature of   9   : Variable
Thickness of   9   : Solve, marginal ray height = 0.00000
Semi Diam   9      : Fixed

INDEX OF REFRACTION DATA:

Surf      Glass       0.450000    0.500000    0.550000    0.600000    0.650000
   0                1.00000000  1.00000000  1.00000000  1.00000000  1.00000000
   1                1.00000000  1.00000000  1.00000000  1.00000000  1.00000000
   2     LAFN21     1.80620521  1.79788762  1.79184804  1.78728036  1.78370773
   3                1.00000000  1.00000000  1.00000000  1.00000000  1.00000000
   4       SF15     1.72487043  1.71248942  1.70386313  1.69754461  1.69273708
   5                1.00000000  1.00000000  1.00000000  1.00000000  1.00000000
   6                1.00000000  1.00000000  1.00000000  1.00000000  1.00000000
   7         F5     1.62084299  1.61262327  1.60678655  1.60244994  1.59911057
   8     LAFN21     1.80620521  1.79788762  1.79184804  1.78728036  1.78370773
   9                1.00000000  1.00000000  1.00000000  1.00000000  1.00000000
  10                1.00000000  1.00000000  1.00000000  1.00000000  1.00000000
  11                1.00000000  1.00000000  1.00000000  1.00000000  1.00000000

ELEMENT VOLUME DATA:

Units are cubic cm.
Values are only accurate for plane and spherical surfaces.
Element surf   2 to   3 volume :       0.609663
Element surf   4 to   5 volume :       0.272423
Element surf   7 to   8 volume :       0.322578
Element surf   8 to   9 volume :       0.478834
```

Listing B.3.3